THERMAL HYDRAULIC ANALYSIS OF LOW ENRICHED URANIUM (LEU) CORE OF THE GHANA RESEARCH REACTOR- 1 (GHARR- 1)

By

AMOAH, Prince

(10636719)

This thesis is submitted to the Graduate School of Nuclear and Allied Sciences, University of Ghana, Legon

In partial fulfilment of the requirements for the award of the Degree,

MASTER OF PHILOSOPHY

IN

NUCLEAR ENGINEERING.

JULY, 2019

DECLARATION

I hereby declare that except for references to other people's work which have been duly cited and acknowledged, this dissertation is the result of my own research work and that neither part nor whole of it has been presented for another degree in this University or elsewhere.

…….

PRINCE AMOAH

(STUDENT)

DATE:……..

.....	.....
DR. EDWARD SHITSI	DR. EMMANUEL AMPOMAH -AMOAKO
(PRINCIPAL SUPERVISOR)	(CO-SUPERVISOR)
DATE:……	DATE ……

ABSTRACT

Following the core conversion of Ghana's Miniature Neutron Source Reactor (MNSR) from high enriched uranium (HEU) to low enriched uranium (LEU), there has been a change in the fuel composition, fuel, clad and other reactor core parameters. Since, the allowable core power in a nuclear reactor is limited by thermal considerations, this study presents thermal hydraulic analysis of the LEU core of the Ghana research reactor -1(GHARR-1). Neutronic parameters of GHARR -1 with LEU core was modelled and simulated using the Monte Carlo N Particle code (MCNP), the core was modelled into two channels, the hottest pin and the average of the remaining pins. Axial and Radial power peaking factors were computed, as well as reactivity coefficients for transient and steady state analysis. The Program for reactor transients (PARET/ANL) was used to model the core under transient conditions of various reactivity insertions. For lower reactivity insertions of 1.94 mk and 2.1 mk, the reactor powers peaked to 30.2 kW and 34.2 kW. And the coolant temperatures were 52.42 ˚C and 54.24 ˚C respectively, far below the saturation temperature of 100 ˚C at a pressure of 1 atm, hence boiling is not expected to occur. The peak clad and fuel temperatures were found to be 62.73˚C and 63.24 ˚C for 1.94 mk and 65.53 ˚C and 66.10 ˚C for 2.1 mk respectively. These clad and fuel temperatures are far below the melting points of the Zicaloy-4 clad material and UO_2 fuel. Accidental insertion of large reactivity of 6.71 mk was simulated and studied, the coolant temperature was found to be 98.8 ˚C, which is close to the coolant saturation temperature, but boiling of the coolant is not envisaged at such large reactivity insertions. But the clad material and the fuel material will be uncompromised as the peak temperatures determined at such large reactivity insertions were lower than their melting points. The plate temperature code (PLTEMP/ANL) was used to model steady state operation of the core. Safety margins; Onset of Nucleate Boiling Ratio (ONBR), Departure from Nucleate Boiling Ratio (DNBR), and Flow Instability Ratio (FIR) were found to be within the safety margins and hence no boiling crisis will occur in the core. Also there is efficient transfer of heat from the fuel to clad. The temperature drop from fuel meat to clad was found to be very low in the range of 0.50 ˚C to 3.18 ˚C for transients and 0.16 ˚C to 0.34 ˚C under steady state conditions. The

results obtained were found to agree with the available experimental results. Similar trends were observed when HEU and LEU results were compared.

DEDICATION

This work is dedicated to my siblings and my grandmother, the late Joana Mensah.

ACKNOWLEDGEMENTS

I thank the Almighty God for the gift of life and good health to undertake this study.

My heartfelt appreciation goes to Dr. Emmanuel Ampomah- Amoako for his support, expert guidance, encouragement and supervision of the project as well as to Dr. Edward Shitsi, my Principal Supervisor.

Special thanks to my parents and my siblings for their support and encouragements.

Finally, I thank my friends and course mates who in diverse ways have helped me in this study.

TABLE OF CONTENTS

DECLARATION ii
ABSTRACT iii
DEDICATION vi
ACKNOWLEDGEMENTS vii
TABLE OF CONTENTS x
LIST OF FIGURES xi
LIST OF TABLES xii
ABBREVIATIONS xiii
SYMBOLS iii
INTRODUCTION 1
1.1 BACKGROUND 1
1.2 PROBLEM STATEMENT 4
1.3 MAIN OBJECTIVE 4
1.4 SPECIFIC OBJECTIVES 4
1.5 JUSTIFICATION OF WORK. 5
1.6 SCOPE 5
1.7 STRUCTURE OF WORK 5
LITERATURE REVIEW 6
2.1 INTRODUCTION 6
2.2 REACTIVITY COEFFICIENTS 6
2.3 POWER PEAKING FACTOR 8
2.4 HEAT TRANSFER 9
2.4.1 Conduction 9
2.4.2 Convection 10
2.5 HEAT REMOVAL AND TRANSFER IN MNSR 10
2.5.1 Heat Transfer to the Fuel Clad 11
2.6 NATURAL CONVECTION 13
2.6.1 Mechanisms of Natural Convection 13

2.6.2 Conditions Required for Natural Convection 14
2.6.3 Natural Convection Flow in a Nuclear Reactor 15
2.6.4 Mass Flow Rate 15
2.6.5 Steady-State Flow 16
2.6.6 Continuity Equation 16
2.7 FLOW REGIMES 17
2.8 DESCRIPTION OF GHARR -1 21
2.9 LEU and HEU Core 22
2.10 COMPUTER CODES 23
2.10.1 Neutronic Codes 23
2.10.2 Thermal-hydraulic codes 24
2.11 TRANSIENT AND STEADY STATE THERMAL HYDRAULIC ANALYSIS. 25
2.11.1 PARET /ANL 25
2.11.2 PLTEMP/ANL 28
METHODOLOGY 32
3.1 MCNP CODE 32
3.2 REACTIVITY COEFFICIENTS 33
3.2.1 Moderator Temperature Coefficient 33
3.2.2 Moderator Void coefficient 33
3.2.3 Fuel Temperature Coefficient 34
3.3 CALCULATION OF POWER PEAKING FACTORS 34
3.4 DELAYED NEUTRON FRACTION 35
3.5 NEUTRON GENERATION TIME 35
3.6 PLTEMP SIMULATION 36
3.6.1 Maximum Clad and Coolant Temperatures 37
3.6.2 Onset of Nucleate Boiling Ratio (ONBR) 39
3.6.3 Flow Instability Ratio (FIR) 40

3.6.4 Departure of Nucleate Boiling Ratio (DNBR).....40
3.7 PARET SIMULATION 40
RESULTS AND DISCUSSION 42
4.1 POWER PEAKING FACTORS 42
4.2 REACTIVITY COEFFICIENTS. 45
4.3 Transient Analysis 47
4.4 Comparison of PARET output with experimental data. 54
4.5 Comparison of PARET output for LEU and HEU Cores. 56
4.6 Steady state thermal hydraulic analysis 57
RECOMMENDATION AND CONCLUSION 60
5.1 CONCLUSION 60
5.2 RECOMMENDATIONS 60
REFERENCES 62
APPENDICES 71

LIST OF FIGURES

Figure 1.1: Longitudinal section of GHARR-1 core. (MCNP Visual editor) *3*

Figure 1.2: Horizontal Cross section of the GHARR-1 core. (MCNP Visual editor) *3*

Figure 2.1: single fuel rod channel [21] *12*

Figure 3.1: Temperature distribution in fuel and coolant [21]**.** *38*

Figure 3.2: Heat transfer in fuel and fuel clad.[60] *38*

Figure 4.1: Axial Maximum and Average Power Peaking Factors. *42*

Figure 4.2: Axial Average Power Peaking Factors for LEU and HEU cores. *43*

Figure 4.3: Axial Maximum Power Peaking Factors for LEU and HEU cores. *44*

Figure 4.4: Comparison of Maximum, Average and Minimum axial power peaking factors per fuel pin *44*

Figure 4.5: Radial Power Peaking Factor per pin for the 335 fuel pins of the GHAAR-1 Core. *45*

Figure 4.1: Temperature variations for 6.71 mk insertion. *54*

Figure 4.19: Comparison of power profile for PARET and Experimental data of GHARR-1 LEU core. *55*

Figure 4.20: Comparison of Coolant temperature for PARET and Experimental data of GHARR-1 LEU core. *55*

LIST OF TABLES

Table 2.1: Some GHARR -1 Core Characteristics *22*

Table 3.1: Temperature and corresponding densities for water. *33*

Table 3.2: Parameter changes/modifications to MCNP input deck for reactivity coefficients computation *34*

Table 3.3: Modifications in GHARR-1 PARET code.....*41*

Table 4.1: Steady state thermal hydraulic analysis of GHARR-1 with LEU core......*57*

Table 4.2: Comparison of outlet coolant temperatures using PLTEMP *58*

Table 4.3:Comparison of PLTEMP output for HEU and LEU core of GHARR-1.....*59*

ABBREVIATIONS

ANL	Argonne National Laboratory
ANS	American Nuclear Society
CIAE	China Institute of Atomic Energy
DNBR	Departure from Nucleate Boiling Ratio
FIR	Flow Instability Power Ratio
FTC	Fuel Temperature Reactivity Coefficient
FORTRAN	Formula Translator
GAEC	Ghana Atomic Energy Commission
GHARR-1	Ghana Research Reactor-1
HEU	Highly Enriched Uranium
IAEA	International Atomic Energy Commission
LEU	Low Enriched Uranium
LANL	Los Alamos National Laboratory
MCNP	Monte Carlo Neutron Particle
MNSR	Miniature Neutron Source Reactor
MTC	Moderator Temperature Coefficient
NNRI	National Nuclear Research Institute
NIRR-1	Nigeria Research Reactor 1
NIST	National Institute of Standards and Technology
ONBR	Onset of Nucleate Boiling Ratio
PARET	Program for the Analysis of Reactor Transients
PLTEMP	Plate Temperature
PPF	Power Peaking Factors
RTC	Reactivity Temperature Coefficient
RERTR	Reduced Enrichment Research and Test Reactor
SAR	Safety Analysis Report
STAR-CCM+	STAR Computational Continuum Mechanics code

SYMBOLS

N_R	Reynolds number
μ	Absolute Viscosity
B	Geometrical buckling
D	Diffusion coefficient
ΔT	Temperature difference
H	Height of core inlet orifice
T	Temperature
P	Power of the reactor
u	Internal energy
q	Energy flux
$\dot{m}$	Mass Flow Rate
c	Heat capacity
Q	Heat generation rate
G	Energy produced per fission
N	Number of fissionable nuclei per unit volume
σ_f	Microscopic fission cross section of the fuel (cm2)
$\emptyset$	Neutron flux (n/cm^2 sec)
V_f	Volume of the fuel (cm3)
K_{eff}	Neutron Multiplication factor
ρ	Reactivity
β_{eff}	Effective delayed neutron fraction
$\wedge$	Neutron generation time
l_p	Neutron life time

CHAPTER 1

1. INTRODUCTION

1.1 BACKGROUND

Simulation and analysis of reactors using Computer codes is a common practice in accessing the neutronic and thermal behaviour of reactors. These codes enable one to predict certain reactor characteristics and ensure safe operation of the reactor through the numerical analysis of the reactor system. Over the years, Nuclear Scientist and Engineers have used variety of codes to perform thermal hydraulic analysis of Nuclear reactors [1]–[3]. Thermal hydraulic analysis involves evaluation of the heat generated and how it is removed within a system. Nuclear thermal-hydraulic analysis is very important in ensuring effective transfer of heat from the fuel meat through the clad, coolant and pool as a result of the sustained fission chain reaction in the reactor core [4]–[6]. The nuclear fuel, which is made up of radioactive materials, must be kept below certain temperature limits to prevent it from being damaged or compromising its mechanical integrity. Knowledge on the mechanism of cooling the fuel, maximum temperatures of the fuel, clad and coolant during normal reactor operations and accident situations and whether the materials are kept within their respective temperature limits are very crucial in the safe operation of nuclear reactors. It is on this basis that physical and chemical properties of the fuel, coolant and other reactor materials are defined.

Both the transient and steady state analysis of the reactor require the coupling of neutronic and thermal analyses: the neutronic analysis studies the reactor core kinetics and dynamics and the thermal analysis is performed to determine the temperature fields in the reactor core and other safety margins associated with temperature variations [7].

In practice, the allowable core power is limited by the rate at which the heat generated is removed from the fuel to the coolant and also transferred from the coolant to outside the core. Excessive accumulation of heat could result in the degradation of the fuel or a change in state of the fuel and thus the core. Hence, the operational power of the reactor core is limited by thermal considerations.

Knowledge in the thermal hydraulics of a reactor core varies between different reactor types and their core configuration. Research reactors may be classified using the criteria of core power density resulting in the relation between neutron flux and core power.

The Ghana Research Reactor, GHARR-1 is a low power research rector, a Miniature Neutron Source Reactor (MNSR) with a tank-in-pool design similar to the Canadian SLOWPOKE (Safe Low Power Critical Experiment) reactor [8].

The reactor serves the purposes of education, training and conducting research. Following a conversion of the reactor core from Highly Enriched Uranium (HEU) to Low Enriched Uranium (LEU), an increased maximum thermal power level of 34 kW can be generated with an equivalent thermal neutron flux of 1.0×10^{12} n/cm^{2}s. The reactor uses rod-type fuel (335 fuel pins, 15 dummies and 4 tie rods) containing approximately 13% enriched uranium-235 as UO_2 pellets in zircaloy-4 cladding.

A typical fuel pin is 4.3 mm in diameter housed in a 0.6 mm thick clad with each of the 335 fuel elements concentrically arranged in 10 folds in the fuel assembly round a central control rod in a guide tube. The reactivity worth of the control rod is about 7 mk, for a fresh core, an excess reactivity of about 4 mk thus, providing a core shutdown margin of 3 mk of reactivity. The fuel assembly is mounted on a 50 mm thick bottom-Beryllium reflector surrounded by a 100 mm thick annular-Beryllium reflector in addition to a top-shim Beryllium reflector. The quantity of water is 1.5 m3 in the reactor vessel, which functions as a shield against radiation, thermalization of the fast neutrons and for the cooling of the core. A water-filled pool of $30\,m^3$ houses the water-filled reactor vessel. Cooling is attained by natural convection using light water. Although, the small core has a low critical mass, the presence of a negative temperature coefficient of reactivity, which is relatively large, has the capacity to boost the inherent safety properties of the core. The smallness in dimensions of the core, leads to the escape and leakage of neutrons in both radial and axial directions which is minimized by the beryllium reflectors around the core. A schematic diagram of the longitudinal and horizontal cross sections reactor is shown in figures 1.1 and 1.2 respectively.

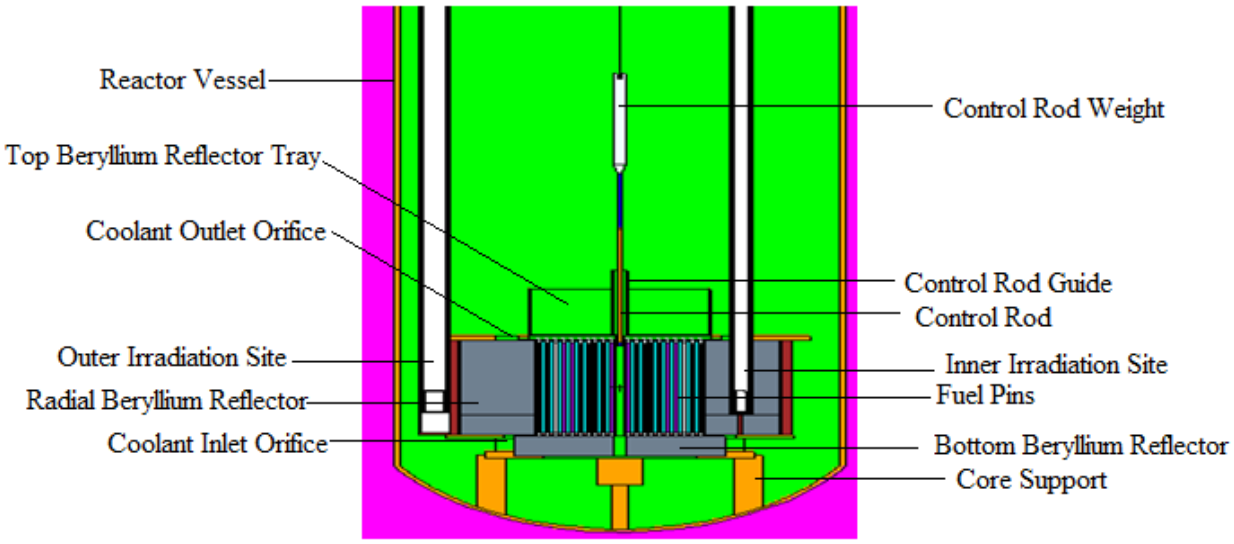

Figure 1.1: Longitudinal section of GHARR-1 core. (MCNP Visual editor)

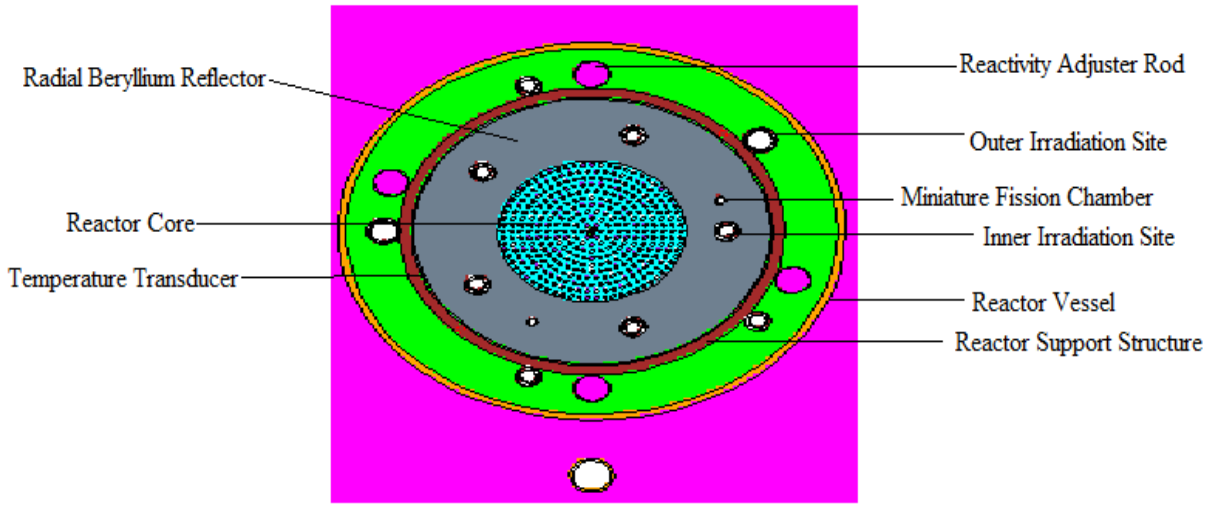

Figure 1.2: Horizontal Cross section of the GHARR-1 core. (MCNP Visual editor)

1.2 PROBLEM STATEMENT

The core conversion of Ghana's MNSR, GHARR -1, from HEU to LEU has led to a change in the fuel composition, fuel clad and other reactor core parameters. Several thermal hydraulic studies have been conducted on the previous GHARR-1 HEU core compared to the few studies performed on the proposed LEU cores to help in understanding the design and operating conditions of the two different HEU and LEU cores. Since, the allowable core power in a nuclear reactor is limited by thermal considerations, there is the need to obtain more thermal-hydraulic data on the new LEU core using thermal-hydraulic codes in order to ensure safe operation of GHARR-1 with the LEU core by the determination of reactor safety margins. There is also the need to predict the thermal behaviour of the reactor core at accident conditions of large reactivity insertions.

1.3 MAIN OBJECTIVE

The main objective of the study is to conduct thermal-hydraulic analysis of Low-Enriched-Uranium (LEU) core of Ghana Research Reactor-1 (GHARR-1) using PARET/ANL and PLTEMP/ANL codes.

1.4 SPECIFIC OBJECTIVES

The specific objectives of the study are as follows:

- To determine the Moderator Temperature coefficient, Void coefficient, Fuel Temperature coefficient and Power Peaking Factors for LEU core using MCNP code.
- To perform thermal hydraulics analysis of LEU core using PARET and PLTEMP codes.

1.5 JUSTIFICATION OF WORK.

Safety in the operation of nuclear reactors is of keen interest to the nuclear industry. Following the core conversion of Ghana's MNSR from high enriched uranium to LEU, there has been a change in the configuration of the core, which may affect variation in the temperature and heat distribution in the core.

This study, which focuses on the thermal hydraulic analysis of the LEU core of GHARR1, will go a long way in ensuring safe operation of the reactor. This work will provide more thermal-hydraulic data on the operation of the LEU core. Data generated could be used as an input into the Safety Analysis Report (SAR) of GHARR-1.

1.6 SCOPE

This work covers thermal hydraulic analysis of GHARR-1 with LEU core using PLTEMP/ANL and PARET/ANL codes. The single phase flow regime is considered in this work as the coolant temperature rise in the core is below the coolant saturation temperature.

1.7 STRUCTURE OF WORK

Chapter one is an introduction to the work. It also looks at the problem statement, the objectives and the justification for this work. Chapter two contains the literature review which generally looks at what research work has already been done in the field of thermal hydraulic analysis and safety analysis and the fundamental theory and parameters used in developing the codes. Chapter three focuses on the methodology used in solving the problem. The applications of the codes MCNP5/ANL, PARET/ANL and PLTEMP/ANL codes in determining and predicting parameters described in chapter two is outlined. And also how the output of one code is used in another code. The results obtained from the study are presented and discussed in Chapter 4. Chapter 5 gives the concluding remarks about the study and recommendations for further studies.

CHAPTER 2

2. LITERATURE REVIEW

2.1 INTRODUCTION

A nuclear reactor is a device or system containing fissionable and fertile materials, carefully arranged so that the nuclear fission chain reaction can be controlled. Aside the sub-atomic particles and fission products, the fission chain reaction yields a lot of energy in the form of heat. This energy must be effectively removed or harnessed as in a research reactor or power reactor respectively. The accumulation of this heat within the core, has serious effects on the control of the reactor and its safe operation [9]. The nuclear fuel, which comprises various radionuclides, needs to be kept at certain temperature threshold, to prevent it from being damaged or compromising its mechanical integrity. Knowledge on the mechanism of cooling the fuel, peak temperatures of the coolant, fuel and clad during normal reactor operations and simulated accident situations and whether the materials are kept within their respective temperature limits are very crucial in the safe operation of nuclear reactors [10] [11]. The effectiveness of heat removal by the coolant is influenced by the properties of the fluid used. This knowledge helps in keeping the temperature of the materials within their corresponding limits of safety.

The amount of heat generated and removed by the cooling system affects the amount of reactivity in the core at any given time. The fractional change in the neutron population in the core from one generation to the other is termed as the Reactivity, as the neutron population increases within the core, more fissions occur and hence more heat generated. The amount of reactivity in the core is affected by some parameters within the core. These parameters are called reactivity coefficients.

2.2 REACTIVITY COEFFICIENTS

When the reactor is operating at an initial power (P_0), any change in P_0 will generally alter the temperatures of the fuel, moderator and coolant. A change in the temperature of any of these components will cause a change in reactivity and this will consequently affect the

operating conditions of the reactor. The reactivity is affected by many factors; power depletion, poisons, fuel depletion, pressure, temperature, etc.

In order to measure the consequence that a deviation in a parameter will have on the reactivity of the core, **Reactivity Coefficients** are implored.

Reactivity Coefficient is the measure of the change in reactivity for a given change in a reactor core parameter. Reactivity coefficients are generally symbolized by $\boldsymbol{\alpha_x}$, where x represents the variable reactor parameter that affects reactivity.

Mathematically, Reactivity coefficient is $\alpha_x = \frac{\Delta \boldsymbol{\rho}}{\Delta \boldsymbol{x}}$ *Eqn 2.1*

For an increase in the parameter x, if there is a corresponding increase in the reactivity, then the coefficient of reactivity will be positive, but if an increase in the parameter x decreases the reactivity of the core, the reactivity coefficient is negative [12]–[14]. Subsequently, reactivity coefficients varies as the core ages. In transient analysis, ranges of coefficients are employed to analyze the response of the reactor during the core life time.

2.2.1 Fuel Temperature (Doppler) Coefficient

The change in the reactivity for a degree change in effective fuel temperature fuel is the fuel temperature coefficient, and is mainly a measure of the Doppler broadening of U-238 and Pu-240 [15], [16]. A rise in fuel temperature increases the effective resonance absorption cross-sections of the fuel and produces an analogous reduction in reactivity.

2.2.2 Moderator Temperature Coefficient

The variation in the reactivity as a result of moderator temperature change per degrees is the moderator coefficient of reactivity. A rise in the temperature of the coolant at a constant density leads to an increase in the absorption of U-238, Pu-240 and other isotopes in the resonance region owing to the hardened neutron spectrum [12], [17]. There is a decline in the fission to capture ratio in the nuclides, U-235 and Pu-239, as a result of the

hardened neutron spectrum. The moderator coefficient gains a more negative value as a result of these effects.

2.2.3 Void Coefficient

Void coefficient is the variation observed in the reactivity per fraction of void change in the reactor. It quantifies how much the reactivity of a nuclear reactor changes as voids increase or decrease in the reactor. Usually, steam bubbles form in the coolant and attach themselves to the walls of the fuel rod and also in the coolant, these bubbles create air gaps, called voids between the fuel elements and the coolant and hence reducing the efficiency of the heat removal system [18].

2.2.4 Power Coefficient

As the core power varies, the collective effect of moderator temperature, fuel temperature and void coefficients changes for every variation in power. The core power coefficient attains a higher negative value as the fuel burns up [15].

2.3 POWER PEAKING FACTOR

The Power Peaking Factor (PPF), is the ratio between the highest power and the average core power of the assembly and is a key value that dictates the maximum allowable power density of the assembly. In a light water moderated reactor, with some fuel rods of U-235 enrichment, the corner fuel rod nearest to the cruciform water- gap generates the highest power in the assembly. The Power Peaking Factor represents the maximum power factor among all the fuel rod in the assembly. It is a relative power value which is calculated according to Equation 2.2.

$$\text{PPF} = \frac{maximum\ power\ density}{average\ power\ density} \qquad \textit{Equation 2.2}$$

Power Peaking Factor can be either positive or negative, and it clearly shows the power magnitude of each fuel rod.

The power peaking factors for a reactor core can be determined axially or radially depending on the model and the code being used. In this work, the axial and radial power peaking factors were computed from the output of (MCNP5) code simulations. The maximum and average power peaking factors for 21 axial nodes were calculated and used in the PARET/ANL code 21. Also, radial and axial power peaking factors per fuel pin were computed and used in PLTEMP/ANL code.

2.4 HEAT TRANSFER

Heat transfer is the movement of heat energy from one point to another. A comprehensive study of the transfer of heat mechanism in any system provides information on the thermal limitations in the design of the system and devices that essentially accomplish the transfer of heat. The major means of heat transfer are:

- Conduction
- Convection
- Radiation

For a given medium or system, the distribution of temperature is governed by the combined effect of the transfer of heat via the three modes. Majority of situations, one mode controls the transfer of heat energy within the system. In such a system, the distributions of the temperature and heat fluxes in the system can be computed by only factoring that mode. Generally, the transfer of heat can be a multi-dimensional time-dependent phenomenon [19].

2.4.1 Conduction

Conduction is the transfer of heat energy in solid materials or the transfer of energy through the vibration of the constituents or atoms in the solid material. In nuclear reactors, conduction of heat occurs between the fuel and the clad as a result of the vibrations of the particles in the clad. An effective transfer of heat from the fuel to the clad is necessary to prevent the build-up of heat in the fuel. It is therefore necessary to know the peak fuel and

clad temperatures and thermal properties of the fuel and clad materials to ensure the safe operation of the reactor [20].

2.4.2 Convection

The transfer of heat energy through fluids is termed convection. Heat is carried away from the surface it interacts with or deposited on the surfaces the flowing fluid encounters owing to the temperature variation present. Convection is categorised mainly under two types; forced convection and natural convection. Forced convection occurs when, the fluid carrying away the heat is pumped by some artificial systems or the fluid is compelled by some mechanism other than thermal contrasts at the surface. For Natural convection, flow of the liquid is as a result of thermal contrasts or temperature variations of the heated surface and the liquid [19].

2.5 HEAT REMOVAL AND TRANSFER IN MNSR

In nuclear reactors, thermal energy is produced as a result of the fission process and also in a much smaller quantity due to the non-fission neutron capture in the fuel, moderator, coolant and other reactor materials. For MNSRs, all the heat generated must be effectively removed to ensure a stable reactor operating power and to sustain the mechanical integrity of the fuel and other reactor components. The smallest integral fuel bearing component of a nuclear reactor is the fuel element. Heat generated by fission consists almost entirely of fission fragments and beta particles and is released in the fuel material. This can be represented mathematically by the following equation:

$$Q = GN\sigma_f \emptyset V_f \qquad \textit{Equation 2.3}$$

Q - the heat generation rate ($W/$ sec)

G - Energy produced per fission (W/fission)

N - Number of fissionable nuclei per unit volume (atoms/cm^3)

σ_f – Microscopic fission cross section of the fuel meat (cm^2)

$\emptyset$ – Neutron flux (n/cm^2 sec)

V_f – Volume of the fuel meat (cm^3) [21]

Heat transfer within the fuel pellet is described by the steady state Fourier equation [22]. For 3 - dimensional flow in the radial direction:

$$q'' = -k\frac{dT}{dr} = -k\nabla T \qquad \textit{Equation 2.4}$$

Where;

q'' – Heat flux (w/m^2)

k - Thermal conductivity of the fuel pellet $(w/m.K)$

$\frac{dT}{dr}$ - Temperature gradient (K/m)

The steady state heat balance can be written as:

$$\nabla^2 T + \frac{q}{k} = v C_P \frac{\partial T}{\partial t} \qquad \textit{Equation 2.5}$$

Where:

T - Temperature (K)

q - Energy generated per unit volume of the fuel meat.

k - Thermal conductivity of the fuel pellet $(w/m.K)$

v - Material density

C_P - Heat capacity of the pellet

$\frac{dT}{dr}$ –Temperature gradient (K/m) [8]

2.5.1 Heat Transfer to the Fuel Clad

The transfer of the energy generated in the fuel is accomplished by conduction. The heat transfer is through the fuel across the boundary between the fuel and cladding and via the cladding to the cladding surface. A schematic diagram of a channel with a single rod is shown in figure 2.1.

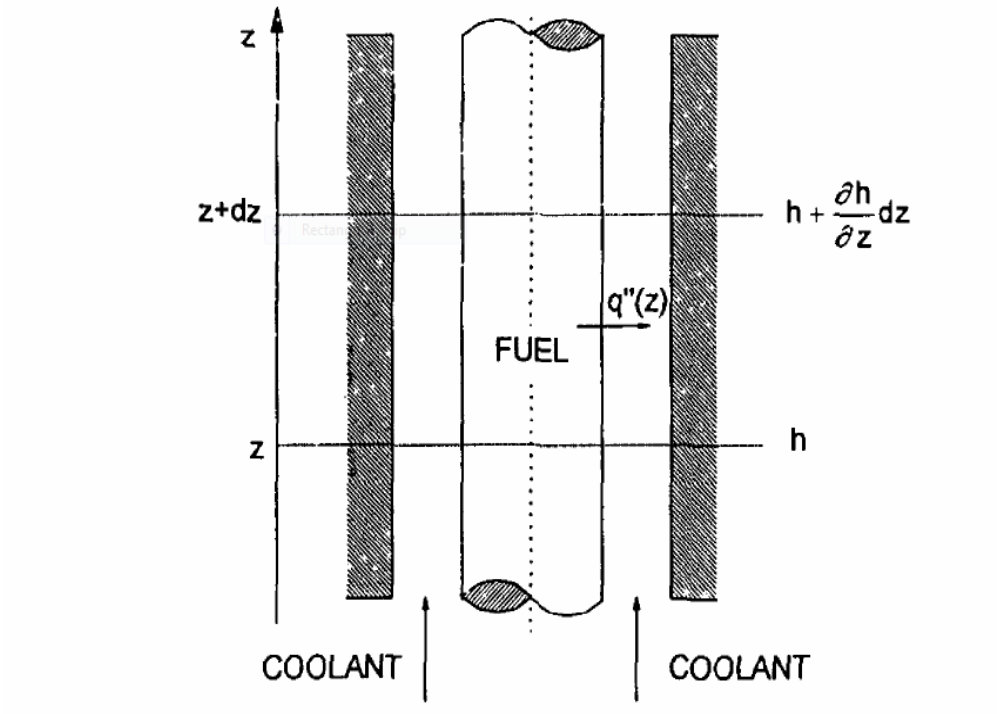

Figure 2.1: single fuel rod channel [21]

Heat conduction in the cladding is given by:

$$\frac{1}{r}k_c\frac{\partial}{\partial r}\left(r\frac{\partial t}{\partial r}\right)=\frac{\partial}{\partial \tau}h(\rho_c c_c t) \qquad \textit{Equation 2.6}$$

Where:

r = the Radius of the fuel meat

k_c = the Conductivity of the cladding $(w/m.K)$

τ = the Time (sec)

p_c = the Specific mass of the cladding (kg/m^3)

c_c = the Specific Heat (J/kg)

t = the Temperature of the clad (K)

h = the Specific Enthalpy (KJ/kg)

Heat convection at the cladding surface is given by:

$$-k_c(\frac{\partial t_c}{\partial r})=h_c(t_c(r_c)-t) \qquad \text{Equation 2.7}$$

Where:

$h_c =$ the Convective heat transfer coefficient (W/m^2K)

$t_c(r_c)$ = the temperature of cladding outer surface (K)

t = the Coolant Temperature (K)

$r_c =$ the Radius of the fuel element (m)

Heat Transfer at the fuel-cladding interface is also given by:

$q'' = h_g(t_f(r_c) - t_c(r_c)$ Where:

$h_g =$ the Gap conductance (W/m^2K)

$t_f(r_c)$ = the Temperature at the surface of the fuel (K)

$f_c(\gamma_c)$ = the Temperature at the inner surface of the cladding (K)

2.6 NATURAL CONVECTION

In natural convection, the movement of the fluid happens without any artificial system such as pumps etc., rather it occurs as a result of density variations, that is buoyancy. In Natural convection, the heat transfer coefficient is relatively low because the flow rate of the fluid connected with natural convection is slightly high [23].

2.6.1 Mechanisms of Natural Convection

Consider a hot object exposed to cold air. The temperature of the outside of the object will drop (as a result of heat transfer with cold air), and the temperature of adjacent air to the object will rise. Consequently, the object is surrounded with a thin layer of warmer air and heat will be transferred from this layer to the outer layers of air.

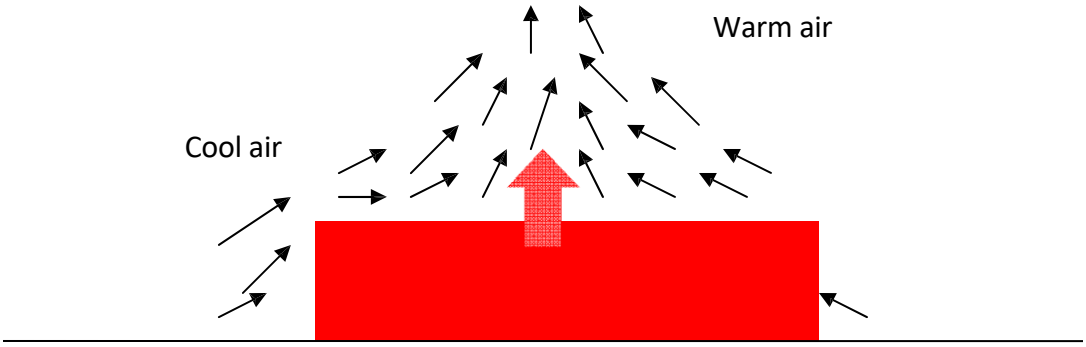

Figure 2.2: fluid flow pattern for natural convection.

The air adjacent to the hot material rises due to a drop in its density, caused by an increase in the temperature of the adjacent air. Cold air replaces the rising warm air, this circulation pattern is the natural convection current. The force that accounts for the rise of the warm air is the buoyancy.

Buoyancy is the force in a gravitational field that raises a light fluid mixed in a heavier fluid. Buoyancy varies directly with the temperature gradient, hence when the drop in temperature between the liquid and the body increases, the buoyancy force will increase as well. For steady conditions, matching the buoyant and the force of friction establishes the air flow rate driven by buoyancy [24].

2.6.2 Conditions Required for Natural Convection

Natural convection occurs when the right conditions exist. If natural circulation begins, and there is the removal of any one of these conditions, natural convection will stop. For natural convection to occur, the following conditions are required:

- A temperature gradient, which is difference in temperature exists (the existence of a heat source and heat sink).
- The elevation of the heat source is lower than the heat sink.
- There is contact between the fluids [23].

2.6.3 Natural Convection Flow in a Nuclear Reactor

Cooling for most pool-type reactors and also for spent or irradiated fuel bundles deposited in pools of water having been removed from the reactor core is through Natural convection. The heat source and sink for a nuclear reactor are the fuel assembly and the water/coolant respectively. Water at the base of the fuel assembly cools the assembly by absorbing the heat energy produced by the assembly [25], [26] . The temperature of the water increases and this results in a decrease in the density of the water. Gravity draws denser light water to the base of the fuel channel to substitute the rising less dense light water in the core. This occurs as a result of the drop in density of the light water surrounding the fuel assembly. As a result of the drop in density of the water, gravity draws cooler water into the base of the assembly replacing the warmer water. The warmer water rises up along the fuel channel. As the warm water moves up the length of the fuel assembly, it gains more energy by absorption hence decreasing more and more in density and thereby becoming lighter and lighter. This leads to it being forced upwards by more cold water moving to the base of the fuel assembly. The cycle is repeated for the cold water and it also absorbs energy, gets heated and thus less dense and rises up, this enhances flow by natural circulation to continue. Water leaving the top of the fuel channel transfers the heat energy through the mixing of it with the remaining light water in the reactor pool. For the natural circulation flow to continue, the temperature gradient must be kept stable. GHARR-1 employs natural convection flow to transfer heat from the clad to the coolant and to the pool water.

Convective heat transfer from the clad to the coolant is described by Newton's law of cooling.

$$\ddot{q} = h_s \Delta T \qquad \textit{Equation 2.8}$$

Where ΔT = the difference in temperature between clad surface and coolant,

h_s is the surface heat transfer coefficient.

2.6.4 Mass Flow Rate

The *mass flow rate* ($\dot{m}$) quantifies the amount of fluid passing a point in at a particular time. Mathematically, the mass flow rate is given by the relation;

$$\dot{m} = \rho A v \qquad \textit{Equation 2.9}$$

ρ = density of the fluid,

A = cross sectional area and v is the velocity of the flow [19].

2.6.5 Steady-State Flow

When the fluid characteristics at any particular point in a given system does not differ over time, such flow is categorized as Steady-state flow. Temperature, pressure, and velocity are key examples of fluid characteristics. For a steady-state flow system, there is no build-up of mass inside any of the constituents in the system [29].

2.6.6 Continuity Equation

The mathematical equation that governs the principle of conservation of mass, momentum and energy is in any system is the continuity equation. For a single inlet and a single outlet of a control system, the mass conservation principle states that, the mass flow rate into the system must be equivalent to the mass flow rate out of the system for steady-state flow. The continuity equation is given by;

$$\dot{m}_{inlet} = \dot{m}_{outlet} \qquad \textit{Equation 2.10}$$

$$(\rho A v)_{inlet} = (\rho A v)_{outlet} \qquad \textit{Equation 2.11}$$

For multiple inlets and outlets of a control volume, the conservation of mass means, the sum of flow rates at all the inlets, is equivalent to the sum of the mass flow rates exiting the control volume.

$$\sum \dot{m}_{inlet} = \sum \dot{m}_{outlet} \qquad \textit{Equation 2.12}$$

The Energy Conservation principle “states that energy cannot be created or destroyed”. The continuity equation for energy flow is expressed as:

$$\frac{\partial \mathrm{u}}{\partial \mathrm{t}} + \nabla \cdot \mathrm{q} = 0 \qquad \textit{Equation 2.13}$$

Where,

- u = internal energy density (energy per unit volume),
- q = energy flux (transfer of energy per unit cross-sectional area per unit time) expressed as a vector,

$$\frac{\partial u}{\partial x} + \frac{\partial v}{\partial y} = 0, \quad \text{Equation 2.14}$$

For the conservation of Momentum:

$$\rho\left(u\frac{\partial u}{\partial x} + v\frac{\partial u}{\partial y}\right) = -\frac{\partial P}{\partial x} + \mu\left(\frac{\partial^2 u}{\partial x^2} + \frac{\partial^2 u}{\partial y^2}\right), \quad \text{Equation 2.15}$$

$$\rho\left(u\frac{\partial v}{\partial x} + v\frac{\partial v}{\partial y}\right) = -\frac{\partial P}{\partial y} + \mu\left(\frac{\partial^2 v}{\partial x^2} + \frac{\partial^2 v}{\partial y^2}\right), \quad \text{Equation 2.16}$$

Where the first term on the right hand side in Eqns. 2.15 and 2.16 refers to pressure forces, $\nabla \cdot P$. and $v = (u, v)$ is the velocity field. The remaining right hand side terms describes viscous forces, $\mu\nabla^2 v$. The left hand side terms represent the change in momentum that any element experiences as it moves between regions of different velocity in the flow field. This has the dimensions of a force, and is referred to as the inertia force, $\rho v \cdot \nabla v$ [21].

2.7 FLOW REGIMES

Fluid flow is considered in two main regimes or types; laminar flow and turbulent flow. Both the laminar or turbulent flow regime is vital in the design, operation and management of any hydraulic system [30], [31]. The quantum of energy required to maintain the desired flow is dependent on the amount of fluid friction, and the quantum of the energy is influenced by the flow type. Fluid flow is of much importance consideration in the design and operation of Nuclear reactors because it encompasses the transfer of heat to the fluid. The various flow regimes are described in fig 2.3.

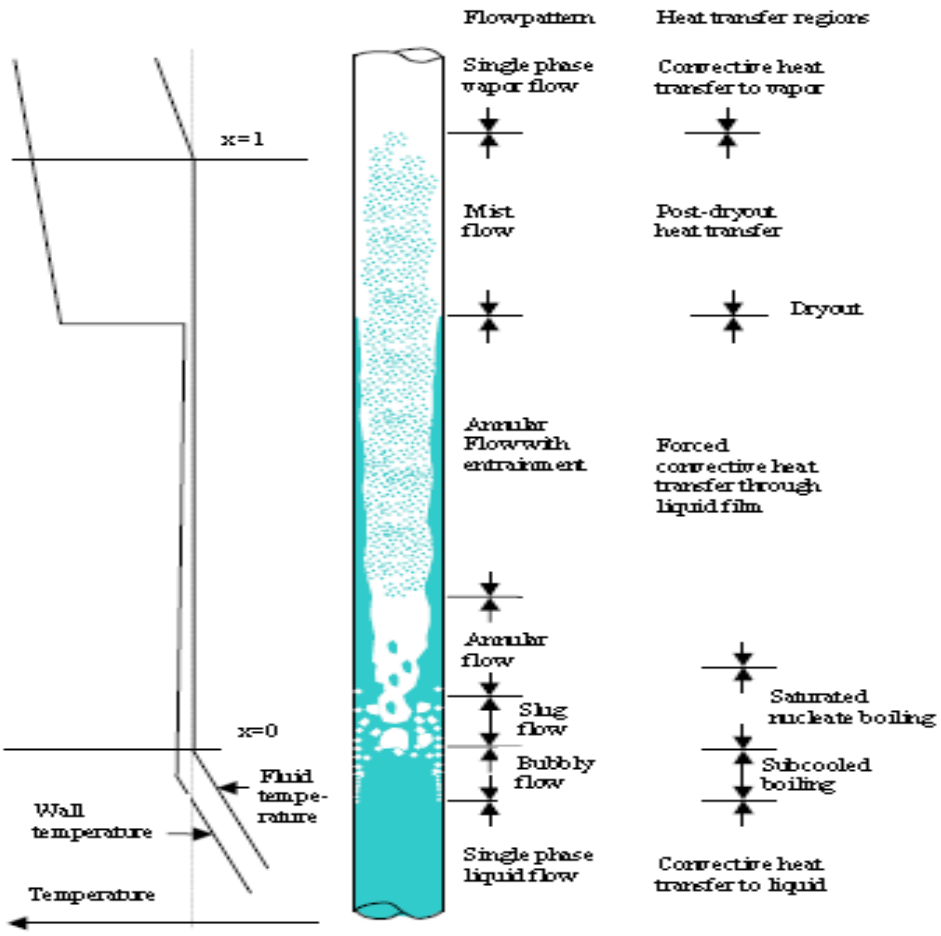

Figure 2.3:Flow regimes in a fluid during heat transfer [19]

2.7.1 Laminar Flow

Laminar flow occurs when layers of the fluid flows over one another at different speeds with virtually no mixing between layers, fluid particles move in definite and observable paths or streamlines. It is also referred to as streamline, drag or viscous flow. These expressions describe the nature of the flow. Viscosity of the fluid plays a significant role in this type of flow, hence the flow is characteristic of viscous fluid. For GHARR-1 operating under normal conditions, flow within the reactor channel is expected to be laminar.

2.7.2 Turbulent Flow

Flow characterised by the irregular or random vibration of particles of the fluid is Turbulent flow. The frequency of the motion of the particles in the fluid is indefinite as there is in wave motion. The motion of the particles is in paths of unequal patterns with no definite layers. In Nuclear reactors, turbulent flow is characterized by power excursions and pressure drops. Safe operation of the reactor is highly compromised under turbulent flow. The inception of turbulence can be predicted by computing the Reynolds number of the flow.

2.7.3 Reynolds Number

Reynolds number (N_R) is the ratio of kinetic energy to viscous damping in a fluid flow The Reynolds number is a dimensionless number consisting of the physical characteristics of the flow. The type of flow either turbulent or laminar is determined by calculating the Reynolds number of the flow. The Reynolds number is calculated using the equation [19];

$$N_R = \rho v D / \mu \qquad \textit{Equation 2.17}$$

With the symbols represented as

N_R = the Reynolds number

v = the average velocity

D = the hydraulic diameter of pipe

μ = the absolute viscosity of fluid

ρ = the fluid mass density

In application, a flow is considered as laminar if the Reynolds number is less than 2000, and turbulent if it is greater than 3500. Transitional flow occurs for Reynolds numbers within the range 2000 and 3500.

2.7.4 Nusselt Number

This is a dimensionless number that compares the heat transferred by convection to the heat transferred by conduction at the heat transfer surface. The component responsible for conduction is determined under the same circumstances the heat convection is measured but with a theoretically static liquid. It is a dimensionless number. A Nusselt number close to unity, that is having similar magnitude of convection and conduction, is characteristic of laminar flow or slug flow . A larger Nusselt number typically in the 100–1000 range corresponds to more active convection, with turbulent flow .

The convection and conduction heat flows are analogous to each other and to the surface normal of the boundary surface, and are all perpendicular to the mean fluid flow.

For natural convection heat transfer coefficient, the Nusselt number is expressed by the Equation 2.18 [19]:

$$Nu = n\,(Gr \cdot Pr)\,m \qquad Equation\ 2.18$$

Gr is the Grashof number; $Gr = g\beta De^3(T_c - \tau_f)/r_f^2$

$g -$ the gravitational acceleration (m/s)

$\beta -$ the volume expansion coefficient $(1/^oC)$

De - the characteristic dimension or equivalent diameter (m)

$r_f -$ Kinematic viscosity of the coolant (m^2/s)

$m -$ Means $T_m = 1/2(T_c - T_f)$ as the calculation of temperature. c and n , as physical properties, depend mainly on the particular geometry as well as the positioning of the solid, the direction of the heat flux as well as the magnitude of Gr.Pr.

CIAE determined the following simple correlation for laminar flow, applicable to the explicit geometry and flow conditions of the MNSR:

$$Nu=n\,(Gr\cdot Pr)^{m} \qquad Equation\ 2.19$$

Where n = 0.68, and m = ¼, when $Gr\cdot Pr < 6 \times 10^6$

Where n = 0.174, and m = 1/3, when $Gr\cdot Pr \geq 6 \times 10^6$

2.8 DESCRIPTION OF GHARR -1

The Ghana Research Reactor, GHARR-1 is a low power research rector, a Miniature Neutron Source Reactor (MNSR) with a tank-in-pool design (Figure 2.4). A maximum thermal power level of 34 kW can be generated with an equivalent thermal neutron flux of 1.0×10^{12} n/cm^{2}s. The reactor uses rod-type fuel (335 fuel pins, 15 dummies and 4 tie rods) containing approximately 13% enriched uranium-235 as UO_2 pellets in zircaloy-4 cladding.

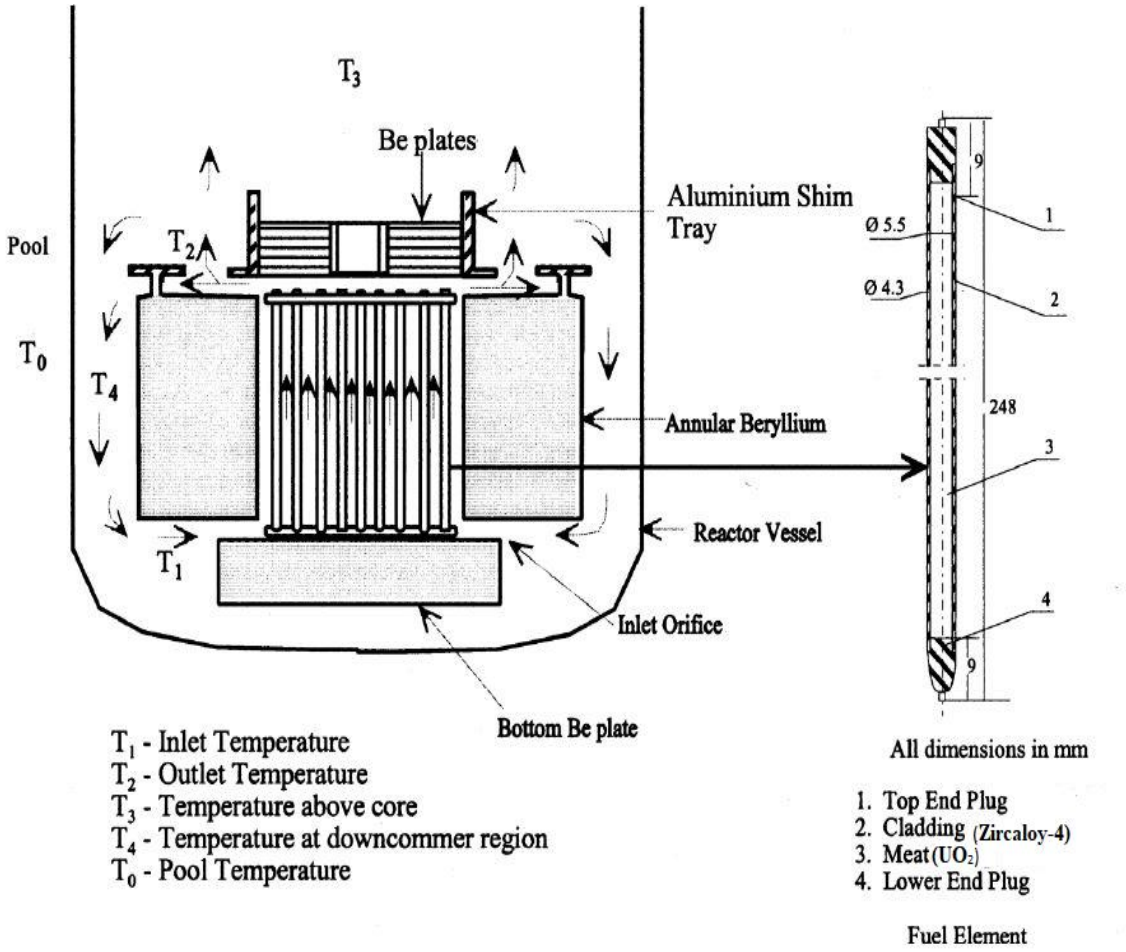

Figure 2.4: A schematic diagram of the coolant flow pattern in GHARR-1 LEU core [32]

A typical fuel pin is 4.3mm in diameter housed in a 0.6mm thick clad with each of the 335 fuel elements concentrically arranged in 10 folds in the fuel assembly with a control rod centrally positioned in the assembly. The fuel assembly is mounted on a 50 mm thick bottom-Beryllium reflector surrounded by a 100 mm thick annular-Beryllium reflector in

addition to a top-shim Beryllium reflector. The quantity of water is 1.5 m^3 in the reactor vessel, which functions as a shield against radiation, thermalization of fast neutrons and for the cooling of the core. Also, heat is removed from the light water in the reactor vessel by virtue of the water-cooling coil situated close to the apex of the reactor. A water-filled pool of 30 m^3 houses the water-filled reactor vessel [32].

Table 2.1: Some GHARR -1 LEU Core Characteristics

Item	Parameter	Value
1	Reactor type	Tank in pool, MNSR
2	Nominal Thermal power	34 KW
3	Fuel type	rod
4	Fuel rod lattice	350
5	Number of Active Fuel rods	335
6	Number of Dummy rods	15
7	Fuel lattice pitch	10.95mm
8	Fuel composition	Uranium Oxide(UO_2)
9	Fuel Density	10.6g/cm-3
10	Dummy element	Zircaloy-4
11	Cladding material	Zircaloy-4
12	U -235 enrichment	13%
13	Active fuel length	230mm
14	Coolant/moderator	Deionised water
15	Coolant inlet temperature	30°C
16	Coolant inlet pressure	1 atm
17	Coolant heat transfer mode	Natural convection
18	Reflector	Beryllium
19	Control rod absorber	cadmium
20	Control rod cladding	Stainless steel
21	Number of control rods	1
22	Core shape	cylindrical
23	Core diameter	230mm
24	Core height	230mm
25	Excess reactivity- cold clean	4mk
26	Maximum thermal neutron flux	1.10×10^{12} n/cm^2s at nominal power
27	Delayed Neutron Fraction	8.57×10^{-3}
28	Prompt neutron lifetime	1.41×10^{-4}s

2.9 LEU and HEU Core

The U.S. Atomic Energy Commission defines a low enriched uranium (LEU) core as a core containing uranium enriched with U-235 isotope less than 20%. The IAEA describes

a nuclide of uranium that cannot be used to make nuclear bombs without further enrichment or transmutation as a low enriched uranium material [33]–[35]. High enriched uranium (HEU) on the other hand is uranium enriched to more than 20% of the U-235 isotope. This type of nuclear fuel is described as weapon grade. Using high enriched nuclear fuel in research reactors, has high risks of nuclear proliferation as well as the diversion or theft of the nuclear material. The lower the enrichment level of any uranium-based nuclear fuel, the higher the plutonium build up, as a result of neutron capture by uranium-238. Hence an optimum composition of uranium that inhibits the build-up of plutonium as well as keeping the uranium fuel unappealing for making nuclear weapons. Generally, the optimum enrichment limit is less than 20%.The LEU of GHARR-1 has an enrichment of 13% of uranium 235 isotope [33], [35]. Also the core life time of LEU cores are expected to be longer than those run by HEU For example, GHARR-1 with HEU was designed for 10 years operation and with beryllium plate adjustments was operated more than 20 years before the HEU core was converted to LEU which is expected to operate for 40 years.

2.10 COMPUTER CODES

Nuclear reactors use computer codes to simulate various reactor operations. These codes are classified in many ways; neutronic codes, thermal hydraulic codes, etc.

2.10.1 Neutronic Codes

Neutronic codes centre their applicability on phenomena that are present in the reactor core. They are capable of predicting reactions between the atoms of materials in the reactor pressure vessel and neutrons or radiation particles, which are the constituents of the fission process (α, β, γ). Through these codes, scientists are able to evaluate the most important parameters, such as the multiplication factor, neutron flux, and isotopic changes in the core fuel or the fuel burn up. Owing to the complexity of the reactor core design (3D), complexity of the calculation process, and the strictly related lengthy calculation time, supercomputers with high computational power play an important role [36]–[38].

Neutronic codes can be divided into a number of types, depending on the problem solving method: deterministic codes or the Monte Carlo method, based on the probability density functions.

Neutronic codes, in various methods, are created to solve the neutron transport equation. This equation is a balance equation for the production and loss of neutrons, through the absorption of neutrons in materials or escape of neutrons from the analysed domain. Examples of the available codes for commercial use, which solve the transport equation through Monte Carlo method, are: Serpent code built by "VTT Technical Research Centre in Finland", "Monte Carlo N-Particle transport Code—MNCP developed by LANL" (with extended version MNCPX) and KENO developed by ORNL code for criticality calculations. The deterministic codes are DRAGON 4 created at the Ecole Polytechnique de Montreal, WIMS and APOLLO-2 developed by the ANL and CEA of France. The MCNP has been used for several studies of GHARR-1 with HEU core [8], [39] and would be used in this work for calculation of some neutronic parameters.

2.10.2 Thermal-hydraulic codes

Thermal hydraulic codes are very important codes for the safety analysis of nuclear reactors. Analyses are done on the steady and transient operational states of the reactor. These analyses are able to predict if with the available safety systems, the reactor will be able to withstand an accident event and the potential consequences of an accident with a related timescale [36], [40], [41]. The simulation results play a key role in designing, licensing and operating the nuclear reactor. These codes are required because nuclear reactor systems work at a highly sophisticated level that surpasses the capabilities of the human mind and simple and basic theoretical models.

In using thermal hydraulic codes for safety analysis there is the need for adequate verification and validation. Verification describes the accuracy of the translation of physical equations to the computer code language, the correctness of the mathematical models, which have to be a realistic representation of the system. Validation is usually performed by comparing the results obtained from the model and experiments. Some

examples of thermal-hydraulic codes include STAR-CCM ++, PARET ANL, PLTEMP ANL, RELAPS and many others.

2.11 TRANSIENT AND STEADY STATE THERMAL HYDRAULIC ANALYSIS.

Transient denotes to any significant deviation from normal operating conditions of reactor parameters relative to time. Reactor transients are characterised into four groups; Very slow transient, a typical example is fuel burn up or depletion with time which occurs with a time constant in several years. Slow transients have a time constant in order of hours; the accumulation of xenon and samarium is an example of this type of transient. Normal transients have a time constant in seconds, such as fuel and moderator temperature change. Fast transients like the drop in control rod or withdrawal at a fast rate (in seconds) [4], [12].

A steady state reactor is a reactor operating at constant power. All the excess heat generated above the steady state condition is removed promptly by passing a fluid through the core and other areas where heat is generated. The characteristics and behaviour of the coolant system are crucially considered in nuclear reactor design [14]. The rate of heat removal from the reactor to maintain a maximum steady state operation time is largely affected by the inlet flow orifice, which in turn determines the temperature effect.

Transient analysis and steady state thermal hydraulic analysis of GHARR -1 with LEU is studied in this work using PARET /ANL and PLTEMP/ANL

2.11.1 PARET /ANL

PARET/ANL is the acronym for Program for the Analysis of Reactor Transients/Argonne National Laboratory. The PARET code has been adapted by the Reduced Enrichment Research and Test Reactor (RERTR) Program to provide transient thermal-hydraulics analysis for research and test reactors with both plate-type and pin-type fuel assemblies [42], [43]. The code has been adapted by the IAEA for testing transient behaviour in research reactors, since it offers a coupled point kinetics and thermal hydrodynamic capability for estimating thermal hydraulic margins [11], [44]. The RERTR Program

conducted studies on the transient analysis of Miniature Neutron Source Reactors using the PARET code [45]. The methodology for both neutronic and thermal-hydraulic analysis has been improved in the PARET/ANL version 7.3 to analyse the transient features of these reactors for both plate-type and pin-type fuel. It has been used for conversion studies in many research reactors in backing the licensing of the reactor [43], [7], [46], [47], [48].

The hydrodynamic solution in the code is based on a Modified Integrated Model [49]. The conservation equations are expressed as:

$$\frac{\partial \overline{\rho}}{\partial t} = -\frac{\partial G}{\partial z} \qquad \textit{Equation 2.18}$$

$$\frac{\partial G}{\partial r} + \frac{\partial}{\partial z}\left(\frac{G^2}{\rho'}\right) = -\frac{\partial P}{\partial z} - \left(\frac{f}{\rho}\right)\left(\frac{|G|G}{2D_e}\right) - \overline{\rho}g \qquad \textit{Equation 2.20}$$

$$\rho'' \frac{\partial E}{\partial t} + G\frac{\partial E}{\partial z} = q \qquad \textit{Equation 2.21}$$

Where G = mass flowrate, P=pressure, E = enthalpy, f =friction factor, g =gravitational acceleration, q = heat source per unit volume, $\overline{\rho} = \rho_l(1-\alpha) + \rho_v\alpha$ is the average density: $1/\rho' = ((1-\chi)^2/[\rho_l(1-\alpha)]) + (\chi^2/\rho_v\alpha)$ is the momentum density, and $\rho'' = [\rho_l\chi + \rho_v(1-\chi)]\,\partial a/\partial\chi$ is the slip flow density, where ρ_l and ρ_v are the saturated liquid and vapour densities, respectively. PARET code enables the reactor core to be represented by up to four sections with diverse power generation, mass flow rate of coolant and other hydraulic parameters.

Mweetwa et al. [50], used the PARET/ANL code to predict the thermal hydraulic behaviour of the Ghana Research Reactor-1 with HEU core after adding 9.0 mm of beryllium to the top shim tray of the core. The core was analysed for reactivity insertions during normal operations (2.1 mk, 3.0 mk, and 4.0 mk) and accidental insertions (5.0 mk and 6.7mk). After nineteen years of operating GHARR-1, simulated transient responses correlated well with those stated in the safety analysis report (SAR). The results obtained demonstrated that the PARET/ANL code is able to calculate thermal-hydraulic data below reactivity insertion of 5.0mk correctly for longer periods of simulation.

Addo et al. [44] modelled the HEU core of GHARR-1 using PARET/ANL (Version 7.3; 2007) into a two-channel PPF of the GHARR-1 core, to conduct thermal hydraulic analysis for transient reactivity insertions of 2.0 mk to 5.5 mk. Coolant and clad temperatures peaked from (42.95 ◦C - 79.42 ◦C) and (59.18 ◦C - 112.36 ◦C) respectively. The ratio of Departure from nucleate boiling conformed to the thermal hydraulic design standard for MNSRs of which there will be no boiling crisis in the core. Their work presented a thermal hydraulic data that confirmed the inherent safety characteristic of GHARR-1, for which the high negative moderator coefficient restricts power run-away or excursion and subsequently the surge of the clad temperature as a result of heat build-up. The maximum reactivity load limit for the PARET simulation in this work was 5.5 mk. The peak power computed was 163.04 kW. This power excursion lasted for a period of 110 s. Analogous effects were observed for temperature of the coolant and clad for the thermal hydraulic profiles. PARET/ANL was used to calculate the margins of thermal hydraulic safety for GHARR-1 and established that the negative feedback of reactivity from the temperature of the moderator to restrict power excursion within the reactor. It was reported that the peak fuel temperature was below the melting point of U-Al and the peak temperatures of the coolant did not attain the value for sub-cooled boiling to occur in the core.

Transient analysis of the Ghana Research Reactor-1 with an HEU core was studied for reactivity insertions of 2.1 mk, 4 mk and 6.71 mk using the PARET/ANL by Ampomah Amoako et al. [4]. A simulation of the fuel rods and their accompanying coolant channels was obtained. Computations of heat transfer in each fuel rod up to a maximum of 21 axial nodes was carried out. The results obtained were reported to be comparable to experiment and numerical studies conducted which demonstrated that the reactor was safe to operate. A peak power of 54.81 kW and a corresponding outlet temperature of 50.01 ◦C were obtained for a reactivity insertion of 2.1mk as compared to results from experiments of 36 kW and 47.1 ◦C respectively.

Akaho and Maakuu [32] carried out reactivity induced transient simulations for a high enriched uranium core Miniature Neutron Source Reactor. The reactivity transients were studied without scram at an initial power of 3 W. It was observed that the power steadily

increased with time from the low power level and suddenly rose to high peaked values and then trailed by a regular decrease in value owing to the negative feedback effects of temperature. Theoretical results compared well with experimental results obtained. A calculated peak power of 100.8 kW for a reactivity insertion of 4 mk agreed well with the measured value of 100.2 kW. Peak powers for the simulated accident scenarios of large reactivity insertions, 6.71 mk and 9 mk corresponding to replacement of spent fuel with fresh fuel and addition of incorrect thickness of Beryllium trays respectively were reported to be 187.23 kW and 254.3 kW. For these high peak powers associated with these reactivity insertions, it was expected that nucleate boiling would occur within the flow channels of the reactor core.

2.11.2 PLTEMP/ANL

The Plate Temperature (PLTEMP) code is used to compute the steady-state temperature solution for reactors of plate type fuel separated by coolant channels. The code after various developments is able to obtain 2-dimensional steady-state temperature solution for reactors of various fuel geometries.

GHAAR- I which uses a rod type fuel can be simulated using this code. PLTEMP is a FORTRAN program that computes the temperature solution for a steady-state flow for a single fuel assembly or the entire nuclear reactor core. The core is divided into two regions; Fuelled and non-fuelled regions, which are modelled. Coolant channels separate each fuel assembly consisting of one or more plates or rods.

In computing the buoyancy head and frictional pressure drop, the code accounts for;

- The channel - to - channel variation of coolant temperature profiles,
- The axial variation of coolant temperature, density, viscosity, Reynolds number and friction factor.

The hydraulic equations implemented in PLTEMP to solve the rate of natural circulation flow in a fuel assembly are derived below, based on the modified Bernoulli equation,

$$P_1 = P_5 + gp_1L_1 + \left(K_1 + \frac{f_1L_1}{D_{h,1}}\right)\frac{W^2}{2p_1A_1^2} + g\int p_{c,1}(z)\,dz + \frac{K_2W_{c,1}{}^2}{2\overline{p_{c,1}}A_{c,1}^2} + \frac{W_{c,1}{}^2}{2D_{hc,1}A_{c,1}^2}\int\frac{f_{c,1}dz}{p_{c,1}(z)}$$
$$+gp_3L_3 + \left(K_3 + \frac{f_3L_3}{D_{h,3}}\right)\frac{W^2}{2p_3A_3^2} + gp_{ch}L_{ch} \qquad \textit{Equation 2.22}$$

In the equation above, the third, fourth, and fifth terms on the right hand side are the gravity head, minor loss, and pressure drop due to wall shear for axial region 1 respectively. The next three terms in equation are the gravity head, minor loss, and pressure drop due to wall shear for axial region 2. And the subsequent three terms in the equation are the gravity head, minor loss, and pressure drop due to wall shear for axial region 3. The last term in the equation is the gravity head for the chimney.

Assuming that the velocity head exiting from the chimney is fully converted into pressure head (not lost into heat), then

$$P_1 = P_1' + \frac{W^2}{2p_1A_1^2} \qquad \textit{Equation 2.23}$$

$$P_5 = P_5' + \frac{(\sum_j W^{(j)})^2}{2p_{ch}A_{ch}^2} \qquad \textit{Equation 2.24}$$

The coolant temperature and density in the chimney are obtained from the enthalpy h_{ch}.

$$h_{ch} = \frac{\sum_j \sum_k W_{c,k}^{(j)} h(,T_{ex,k}^{(j)})}{\sum_j \sum_k W_{c,k}^{(j)}} \qquad \textit{Equation 2.25}$$

In the steady-state natural circulation, there is no pressure drop at the inlet and exit of the core, this assumes that the frictional pressure drop due to the creeping flow of coolant in the pool is negligible, and that the coolant temperature in the pool is uniformly equal to the inlet temperature over the fuel assembly plus chimney height.

$$P_1 - P_5 = gp_1(L_1 + L_2 + L_3 + L_{ch})\,; P_4 - P_5 = gp_{ch}L_{ch} \qquad \textit{Equation 2.26}$$

The flow rate in a fuel assembly in steady state natural circulation is given by,

$$gp_1(L_2 + L_3) + gL_{ch}(p_1 - p_{ch}) = (K_1 + \frac{f_1L_1}{D_{h,1}})\frac{W^2}{2p_1A_1^2} + g\int p_{c'1}\,(z)dz +$$

$$\frac{K_2W_{c,1}^2}{2\overline{p_{c,1}}A_{c,1}^2} + \frac{W_{c,1}^2}{2D_{hc,1}A_{c,1}^2}\int \frac{f_{c,1}dz}{p_{c,1}(z)} + gp_3L_3 + (K_3 + \frac{f_3L_3}{D_{h,3}})\frac{W^2}{2p_3A_3^2} \qquad \textit{Equation 2.27}$$

Collecting the channel - independent terms in Eqn. 2.23 on the left hand side, we get Eqn. 2.24) for any coolant channel k in the heated section of the assembly.

$$P_2 - P_3 + \frac{W^2}{2p_1A_1^2} - \frac{W^2}{2p_3A_3^2} = g \int p_{c,k}(z)\, dz + \frac{K_2 W_{c,k}{}^2}{2\overline{p_{c,k}}A_{c,k}^2} + \frac{W_{c,k}{}^2}{2D_{hc,k}A_{c,k}^2} \int \frac{f_{c,k}dz}{p_{c,k}(z)}$$

Equation 2.28

for $k = 1, 2, \ldots N_c$

The PLTEMP/ANL code which has been used in this work for steady state analysis, uses for its routine checks, the Babelli-Ishii criterion for excursive flow instability after boiling. The criterion is based on the sub cooling number and the Zuber number.

Odoi et al. [51] studied acceptable safety margins under both normal and accident conditions for a proposed LEU of 348 fuel pins under Steady state, using the PLTEMP/ANL code version 4.1, six hot channel factors were used in the code to calculate reactor safety margins and also calculate the peak coolant and clad surface temperatures by setting the inlet temperature to 30 °C. Other results of thermal-hydraulics analyses for both HEU and LEU cores, such as the minimum onset of nucleate boiling ratio and critical heat flux, were studied in their work. Results for the thermal hydraulics analysis indicates good safety margin for the proposed LEU core.

Jonah et al [52] used PLTEMP /ANL code version 4.1 to study the steady state thermal hydraulics and determine operational limitations and margins of safety for an MNSR with a proposed UO_2 LEU core, with a core configuration of 348 fuel pins and 34 kW as nominal power . Measured data of Nigeria Research Reactor 1(NIRR-I) with the existing HEU core of nominal power 31 kW was used to confirm calculated data. MCNP5 code was used in the computations of the power peaking factors of the fuel rods within the core of the HEU and the proposed LEU core. The model was further calibrated to obtain coolant temperature increase of 13°C from experiment, to model fluid flow resistance for the flow of coolant in the code at a reactor power of 15 KW. Results obtained showed that, the margin to Onset of Nucleate Boiling ratio, compared to the proposed the LEU core reactor power of 34 kW is significantly high and is in good agreement with the equivalent margin for the HEU core. They reported also that, since melting points for the fuel and cladding material for the proposed LEU were higher as well as having high corrosion resistance, the margins of safety are boosted for steady state operation of the proposed NIRR-I with LEU core.

This work made use neutronic of data from a Monte Carlo N Particle Code to obtain the steady state and transient thermal hydraulic data for the GHARR -1 core with LEU using PARET and PLTEMP. Details of the method and expected results from the work are discussed in the next chapter.

CHAPTER 3

3. METHODOLOGY

This chapter presents the methodology adopted to achieve the objective specified in chapter 1. This includes detailed procedure of the computer simulations used to obtain the numerical results in this work.

3.1 MCNP CODE

The Monte Carlo N-Particle Transport Code (MCNP) is a neutronic code for simulating various processes. Los Alamos National Laboratory(LANL) started building this code since 1957 and has undergone several major improvements [53], [54]. The code is used mainly for modelling and simulating nuclear processes as well as model the interactions of particles involving neutrons, photons, and electrons. The code has the ability to track many particles from their time of production throughout its life to till it is absorbed, captured or escapes from the control volume defined. Using transport data, probability distributions are sampled randomly to evaluate the consequence on the particle at each step of its life. MCNP is a well-accepted code in modelling the neutronic behaviour of nuclear reactors because of its ability to model complex three-dimensional geometries and its extensive validation.

Criticality problems in MCNP are simulated using the KCODE card which requires the nominal number of source histories (N) per *cycle*, a preliminary estimate of K_{eff} ,the number of source cycles, (I_c), to skip before K_{eff}| accumulation, active number of cycles (I_A),and the total number of cycles(I_t) [54].

The power peaking factor, reactivity coefficients, delayed neutron fraction and neutron generation time were simulated with the following specifications in the model; N was set at 500,000, K_{eff} was given an initial guess of 1.004, the total number of cycles (I_t)was set as 330 cycles with the first 30 cycles being inactive and the 300 cycles being active. These values were sufficient to provide efficiency and sufficient statistical accuracy in the results. The value for the number of cycles to be skipped was chosen to provide sufficient cycles for statistical convergence of the K_{eff} around a certain solution, allowing for the most accurate neutronic data to be obtained. A total of 300 million particles were used for each simulation.

3.2 REACTIVITY COEFFICIENTS

3.2.1 Moderator Temperature Coefficient

Computation of the moderator temperature reactivity coefficient was done by modifying the temperature value to the corresponding equilibrium energy on the temperature card (tmp) in the MCNP 5 code. The density corresponding to the temperature used was inputted in all cell cards that contain water in the model. The corresponding densities for the temperature values were obtained in literature from the National Institute of Standards and Technology (NIST)[55], [56] as shown in table 3.1 below. The values for K_{eff} were predicted for the temperature range of 30°C to 90°C. The reactivities obtained from the K_{eff} values were plotted against temperature. The relationship between temperature and reactivity was determined using the 3rd order polynomial equation. Equation 3.1 was used to compute the moderator temperature coefficient.

$$\alpha_m = \frac{\Delta \boldsymbol{\rho}}{\Delta \boldsymbol{T}} \qquad \text{Equation 3.1}$$

Where α_m is the moderator reactivity coefficient.

Table 3.1: Temperature and corresponding densities for water.

Temperature (K)	Density (g/ml)
303.1600	0.9956464
313.1600	0.9922125
323.1600	0.9880305
333.1600	0.9831907
343.1600	0.9777589
353.1600	0.9717842
363.1600	0.9653029

3.2.2 Moderator Void coefficient

Modifications were made to the coolant density in the MCNP 5 model. The densities that were used correspond to a temperature range of 30 °C to 90 °C as shown in Table 3.1.

3.2.3 Fuel Temperature Coefficient

The MCNP 5 model was modified by changing the tmp data card of the atoms in the fuel at that temperature in the model to represent the desired temperature. The changes that were made to the TMP data card corresponded to the equilibrium energy of the atoms in the fuel at that temperature. The temperature range 30°Cto 650 °C was used for the MCNP runs to predict the corresponding eigenvalues. A summary of the various parameters that were modified in the MCNP input deck for predicting the multiplication factors corresponding to different temperatures, densities and percent void is presented in Table 3.2.

Table 3.2: Parameter changes/modifications to MCNP input deck for reactivity coefficients computation

Reactivity Coefficients	Temperature Range(°C)	Parameters			
		Fuel Temperature	Core Water Temperature	Fuel Density	Core Water Density
Moderator Temperature coefficient	30-90	Not Modified	modified according to temperature range	Not Modified	Modified according to temperature range
Moderator void coefficient	30-90	Not Modified	Not Modified	Not Modified	Not Modified
Fuel Temperature coefficient	30-650	Modified according to temperature range	Not Modified	Not Modified	Not modified

3.3 CALCULATION OF POWER PEAKING FACTORS

Power Peaking Factors (PPF) for GHARR-1 was calculated by dividing the hottest and cold fuel pins in the core to a maximum of 21 axial segments based on the PARET code [4]. The MCNP code was used to compute the energy (eV) of each segment for an inlet temperature of 30 °C. The core average power was obtained by finding the average of the total core power and the power peaking factor of each particular segment was evaluated by dividing its power by the core average power. Radial power peaking factors were also evaluated from the output of the MCNP code run. The calculated axial and radial power peaking factors were used in the PARET and PLTEMP codes presented in the Appendix.

3.4 DELAYED NEUTRON FRACTION

The fraction of delayed neutrons was predicted using the Prompt method which requires two cases to predict eigenvalues; firstly, the eigenvalue for prompt neutrons k_p only was predicted and in the second case, the eigenvalue combining prompt and delayed neutrons $k_c$was predicted [57]. The TOTNU card with a null entry was used to predict the number of fission neutrons as a result of prompt and delayed neutrons. After which, The TOTNU data card with entry NO was used to obtain the eigenvalue for prompt neutrons only. The TOTNU data card with entry NO prevents the influence of delayed neutrons and thus the multiplicity per fission is due to the average prompt neutron and is computed for all fissionable nuclides with prompt values k_p available.

The values for k_p and K_{eff} obtained were used to compute the delayed neutron fraction using Equation 3.2

$$\beta_{eff} = \frac{k_p - 1}{K_{eff}} \qquad \text{Equation 3.2}$$

3.5 NEUTRON GENERATION TIME

The 1/V absorber method was used to predict the neutron generation time. In this method, all materials in the core were doped with a small amount of a 1/V absorber material. Different concentrations of the doping material are used. The corresponding perturbed eigenvalue for each concentration is given as k_{pt} and the steady state unperturbed eigenvalue is given as k_u.

The 1/V absorber material inserts a negative reactivity which is given as;

$$p = -\frac{\Delta k}{k} = \frac{k_u - k_{pt}}{k_u * k_{pt}} \qquad \text{Equation 3.3}$$

According to Bretscher [57], the negative reactivity inserted can be expressed by Equation 3.4

$$-\frac{\Delta k}{k} = l_p V n \sigma \qquad \text{Equation 3.4}$$

hence, $l_p = \frac{-\frac{\Delta k}{k}}{Vn\sigma}$ Equation 3.5

where l_p is the neutron lifetime,

n is the atomic density of the 1/ V absorber (atoms/b - cm)

V is the speed ofthermal neutrons $= 2.2E5\ cm/s$

σis the absorption cross section of the absorber (B - 10) $= 3837\ b$

The neutron generation time is given as;

$\Lambda = \lim_{n\to 0} l_p = \lim_{n\to 0} \frac{-\frac{\Delta k}{k}}{Vn\sigma}$ Equation 3.6

3.6 PLTEMP SIMULATION

The PLTEMP/ANL code version 4.0 was obtained and modelled to study the steady state thermal hydraulics of GHARR-1 with LEU core. The code is designed for the evaluation of the steady state thermal-hydraulic performance of research reactors in the sub-cooled boiling regime [33], [7]. The input deck used was a modification of the one provided in the spectrum of Core Conversion Coordinated Research Project of the International Atomic Energy Agency (IAEA) and developed at the ANL for testing the application of the code on analysis of the steady state parameters of GHARR-1.

The core of GHARR-1 was modelled for all the 335 fuel pins. The fuel pins were arranged in 12 fuel bundles, with the first 11 bundles containing 30 fuel pins, accounting for 330 fuel pins and the remaining 5 fuel pins were put in the last 12th bundle. The 0303 card which represents the axial power peaking factor per assembly was updated with the maximum power peaking factor value (FZ). This value (NELFI) was repeated 30 times. The power shape corresponding to F_Z was inputted on the 21 heat transfer nodes on card 0701 with each jth node having a relative distance of 0.010952m from the coolant inlet to the assembly.

The radial power peaking factors were inputted in card 0309. A detailed input deck indicating these parameters is presented in the Appendix. Both the axial and radial power peaking factors were obtained from the MCNP simulations of the core.

An initial run was performed for the updated input deck. The inner iteration factor (EPSLNI) on card 0500 was decreased from 0.06 to 0.02, to achieve convergence.
From the PLTEMP simulation steady state safety margins such as the maximum fuel, clad and coolant temperatures, Onset of Nucleate Boiling Ratio (ONBR) departure from nucleate boiling ratio (DNBR), and Flow instability ratio (FIR) were computed.

3.6.1 Maximum Clad and Coolant Temperatures

Under steady state operating conditions, the balanced heat equation is [1], [58]:

$$Q(z) = WC_p[T_f(z) - T_{fn}] \qquad \text{Equation 3.7}$$

Where,

$Q(z)$ − Heat conveyed up along the axial position Z, from the inlet of the core by the coolant.

W − The mass flow rate of the coolant (Kg/s) and

C_p − The Specific heat capacity of the coolant (J/Kg°C)

The temperature distribution for coolant can be found following eqn. 3.7,

$$T_f(z) = T_{f_{ln}} + \frac{Q(z)}{WC_p} = T_{f_{ln}} + \frac{1}{WC_p}\int_{z_m}^{Z} q_l\,(z)dz \qquad \text{Equation 3.8}$$

Where

q_l − power density (linear) at position z, (W/m) ,

T_{f_m} − Inlet temperature of coolant,(°C)

Given τ_{f_m} , w, and $q_l(z)$, temperature distribution in the coolant in the axial direction, T_{f_m} for Eqn. 3.8, temperature of fuel pellet position, $T_{0\ max}$,position, $z_{0\ max}$, maximum cladding surface temperature, $\tau_{c\ max}$, are displayed in the Figure 3.1.

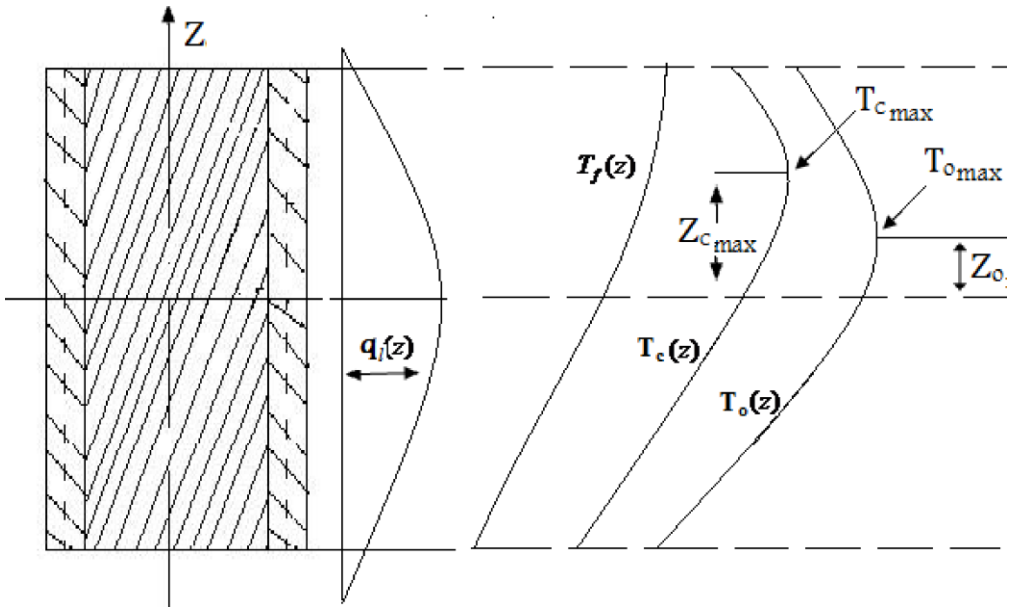

Figure 3.1: Temperature distribution in fuel and coolant [21]**.**

It is expected that the highest value for coolant temperature should occur at the exit of the channel. Also at the central point of the channel, the maximum temperature for the clad outer surface temperature and fuel temperature happens. These values must be kept below their regulatory values to ensure the safe operation of the reactor [51], [59].

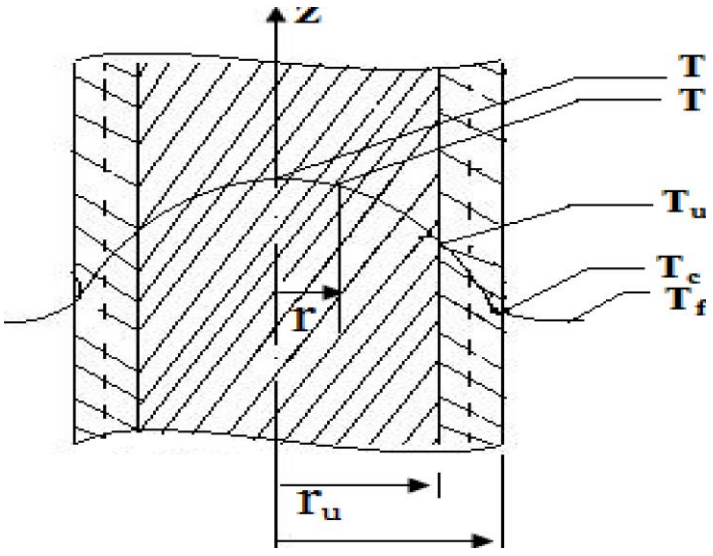

Figure 3.2: Heat transfer in fuel and fuel clad.[60]

$\frac{d^2T}{dr^2} + \frac{1}{r}\frac{dT}{dr} + \frac{q_v}{K_u} = 0$ *Equation 3.9*

Where q_v – heat production rate, W/m^3

K_u – Thermal conductivity of fuel rod, W/m^oC

When q_v is uniformly distributed, Equation 3.9 is solved to get,

$T_o - T_u = \frac{q_v r_u^2}{4K_u} = \frac{qr^u}{2K_u} = \frac{q_l}{4\pi K_u}$ *Equation 3.10*

Where, T_o – fuel rod centre temperature,

T_u – Fuel rod surface Temperature,

r_u – Radius of fuel rod;

q – Surface heat flux,

q_l – Linear power density

$q_l = 2\pi r_u q$ *Equation 3.11*

Heat conduction of cladding

$Q = -K_c F \frac{dT}{dr}$ Fourier law [22], [61] *Equation 3.12*

Solving Equation 3.11, one can obtain

$T_u - T_c = \frac{Q}{2rrK_cL}\ ln\ \frac{r_c}{r_u} = \frac{q_l}{2rrK_c}\ ln\ \frac{r_c}{r_u}$ *Equation 3.13*

Q – Heat transferred through the cladding via conduction (w),

F –Area of surface perpendicular to the direction of conduction

L – Length of fuel rod (m).

3.6.2 Onset of Nucleate Boiling Ratio (ONBR)

This is a ratio that gives the margin by which nucleate boiling will occur. Nucleate boiling occurs when the temperature at the surface of the fluid is greater than the saturated temperature of the entire fluid by a particular margin. In nucleate boiling, the heat flux is below the critical heat flux. For water, this margin has been pitched at 10 ˚C to 30 ˚C. In MNSRs, the value of this ratio is critical because, the onset of nucleate boiling decreases

the heat transfer coefficient of the fluid and also affects the stability of the coolant flow in the reactor.

3.6.3 Flow Instability Ratio (FIR)

It is the ratio of power at the onset of flow instability (OFI) to the nominal power. It is affected by surface roughness, onset of nucleate boiling among others. For a smooth surface the ONB is a major source of flow instability as the formation of bubbles will impede the flow of the coolant. The coolant flow ensures the transfer of heat generated within the core, hence flow instability is undesirable and should be avoided in the operation of the reactor [1], [62].

3.6.4 Departure of Nucleate Boiling Ratio (DNBR)

Nucleate boiling is boiling by the rise and collapsing of bubbles to the surface of the fluid conducting the heat. The ratio of the heat flux at the critical point to the heat flux relative to the prevailing power (actual). The parameter is used to determine the margin to failure by boiling crisis. Also referred to as the critical heat flux ratio. These ratios are computed using the relationship (Equation 3.14) [63].

$$\mathrm{DNBR} = \frac{[\frac{q}{A}]_{DNB}}{[\frac{q}{A}]} = \frac{q'''_{critical}}{q'''_{actual}} \qquad \textit{Equation 3.14}$$

3.7 PARET SIMULATION

The transient studies of GHARR-1 with LEU core was studied using the PARET/ANL code (Version 7.3 of 2007).The PARET/ANL code has undergone several modifications to integrate reactor thermal–hydraulic margins; which include departure from nucleate boiling ratio, flow instability ratio, heat transfer correlations for single and two-phase flow, and flow rates [49] [64]. The code also provides an estimate of voiding formed by sub cooled boiling via its alternate model for voiding. Changes were made to the clean core input deck model of GHARR-1 core. Kinetic parameters obtained from MCNP simulations of GHARR-1 with LEU core were used in the model. Since GHARR -1 has a cylindrical

core, with a cylindrical fuel pin, a cylindrical geometry was selected for this computer code simulation. The total active region of GHARR-1 core was divided into two channels, one channel representing the hottest pin and the other representing the rest of the reactor core that is the average channel. The axial dimensions of these channels were divided into 21 equally spaced regions called the nodes. Reactivity insertions of 1.94 mk, 2.1 mk, 2.99 mk, 3.87 mk, 4.0 mk and 6.71 mk transients were simulated for the core. These insertions were selected to relate with those used in literature and the SAR of GHARR-1. The cards that were modified and the corresponding parameters are described in Table 3.3.

Table 3.3: Modifications in GHARR-1 PARET code

PARET card number	Pneumonic	Parameter and Description.
1003	PF	Volume of fuel meat
	ENTHIN	Inlet temperature
1005	BBEFF	Delayed neutron fraction.
	EL	Prompt neutron life time.
1006	TRANST	Total time investigated for Transient.
1007	GAMMA-0	Constant in fuel temperature feedback equation.($)
	GAMMA-1	Linear coefficient in fuel temperature feedback equation. ($/T)
	GAMMA-2	Quadratic coefficient in fuel temperature feedback equation. ($/T2)
	GAMMA-3	Cubic coefficient in fuel temperature feedback equation. ($/T3)
	GAMMA-4	Temperature offset coefficient in fuel temperature feedback equation.($/T4)
5101 ,5102	DTEMP	Moderator temperature coefficient
	DVOID	Moderator void coefficient
5102-5122	PFQ	Maximum power peaking factors
5202-5222	PFQ	Average power peaking factors
9003-9004	REACC	Reactivity insertions for varying times

Results from the simulations and their implications in the analysis of the reactor are discussed in the next chapter.

CHAPTER 4

4. RESULTS AND DISCUSSION

This chapter presents and discusses the results obtained from the study and how it relates with some experimental data on GHARR-1 with LEU core and previous studies carried out on the GHARR-1 with HEU core.

4.1 POWER PEAKING FACTORS

The axial power peaking factors for 21 axial nodes were calculated from the MCNP 5 run using the thermal energy group. PARET simulations were done using 21 axial nodes for the hottest pin (maximum) and average of the remaining fuel pins. Fig 4.1 shows the relationship between the maximum (hottest pin) and average power peaking factors.

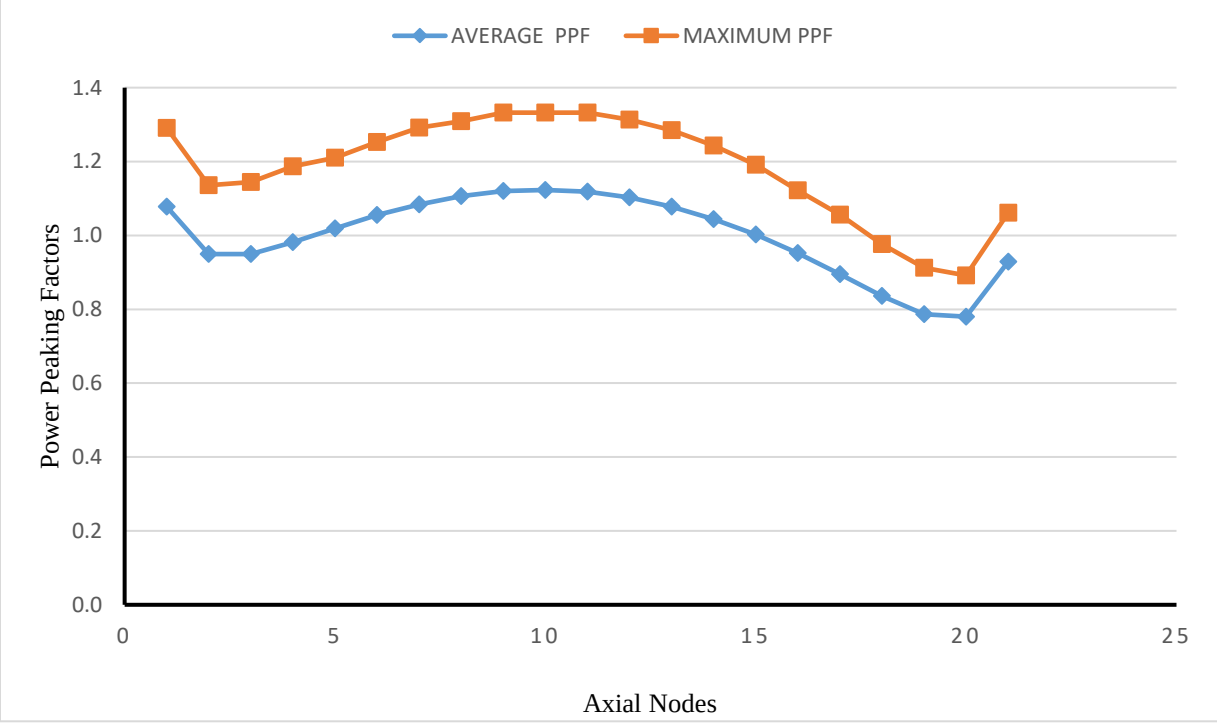

Figure 4.1: Axial Maximum and Average Power Peaking Factors.

Figure 4.1 relates the axial maximum and average power peaking factors of the LEU core of GHARR-1. Maximum values for both axial maximum and average power peaking

factors are found at the center of the core. This is as a result of the presence of water as moderator as well as full withdrawal of the control rod, in addition to the effect of the surrounding beryllium which is maximum around the center accounts for this. As can be observed from figure 4.1, the neutron density starts decreasing axially until it reaches the beryllium reflector where it starts increasing again. The increase in neutron density is due to the presence of beryllium which reflects neutrons into the core. The distribution tilts towards the top of the core for both maximum and average power peaking factors. This is attributed to the higher leakage of neutron at the top because of the top not being heavily reflected with beryllium like the bottom and the annular directions. Both axial maximum and average power peaking factors show a similar power peaking profile. However, the average power peaking factor is lower compared to that of the maximum power peaking factor. The maximum values for both axial maximum and average power peaking factors from figure 4.1 was predicted to be 1.3323 and 1.1229 respectively.

Data for the axial maximum and average power peaking factors for the HEU core was obtained from work by Ampomah- Amoako et al. [4]., a comparison of the axial power peaking factors for both HEU and LEU cores is shown in figures 4.2 and 4.3.

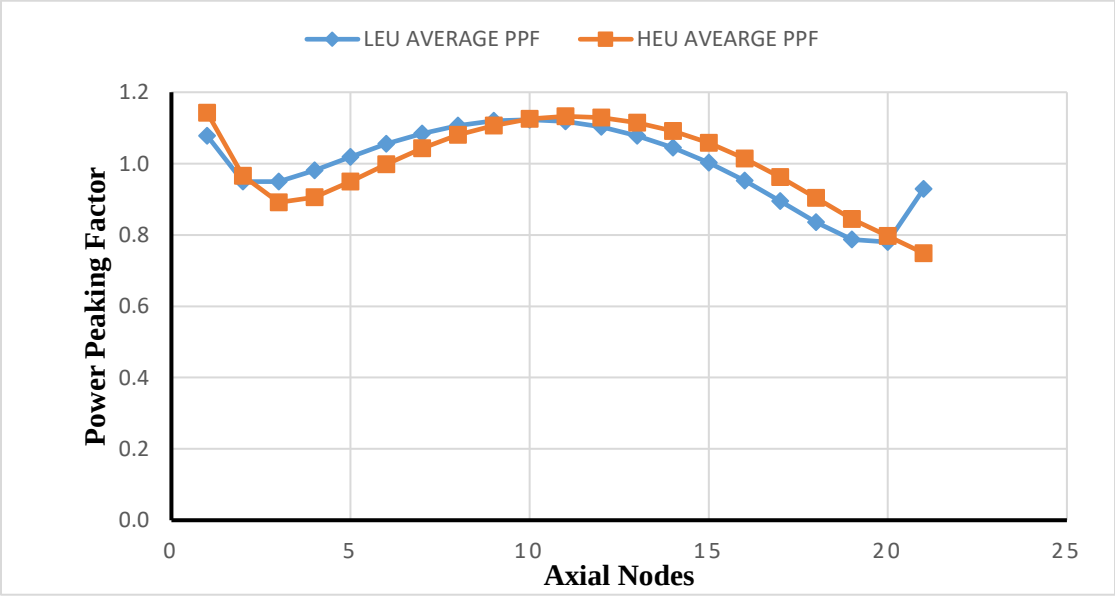

Figure 4.2: Axial Average Power Peaking Factors for LEU and HEU cores.

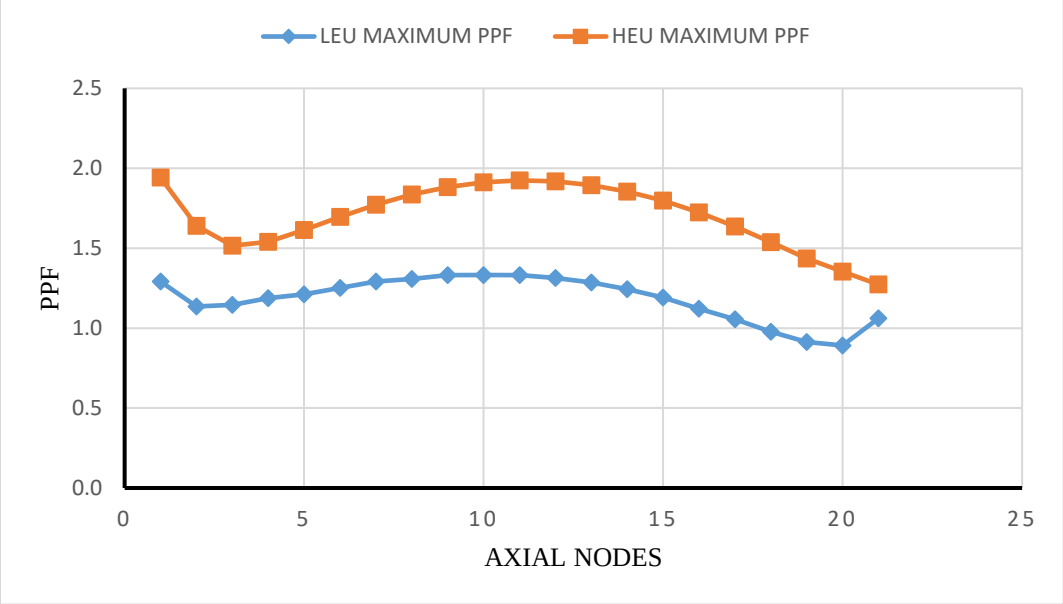

Figure 4.3: Axial Maximum Power Peaking Factors for LEU and HEU cores.

For PLTEMP simulations, axial and radial power peaking factors were calculated per fuel pin. The axial power peaking factors were computed for the minimum, average and maximum values per fuel pin for the whole core. In all 335 fuel pins were modelled. Figure 4.4 compares the average, maximum and minimum axial peaking factor per pin.

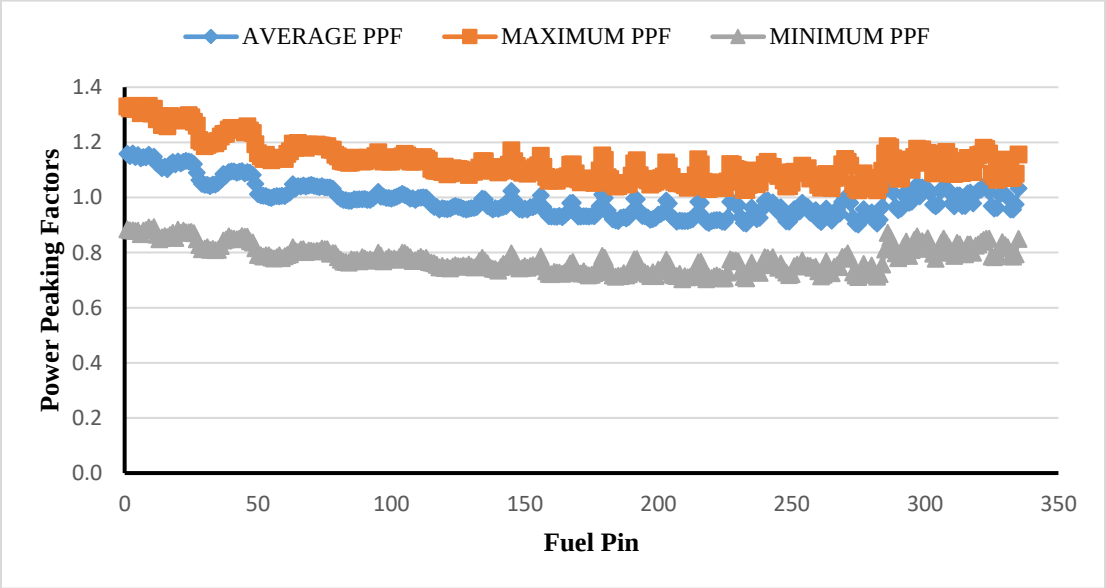

Figure 4.4: Comparison of Maximum, Average and Minimum axial power peaking factors per fuel pin

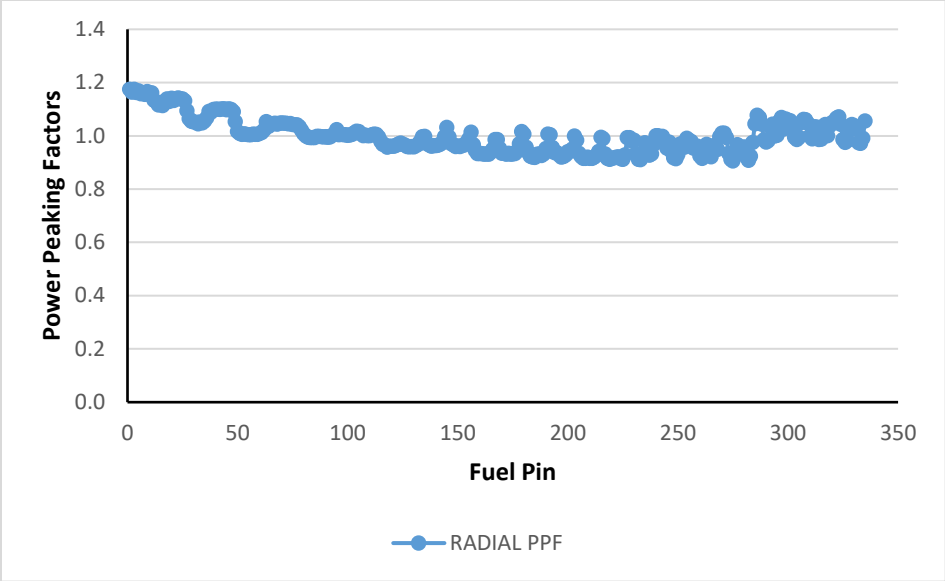

Figure 4.5: Radial Power Peaking Factor per pin for the 335 fuel pins of the GHAAR- 1 Core.

Figure 4.5 presents the radial power distribution in the GHARR-1 LEU core. The power profile is nearly flat indicating the core power stability and reduction of leakage as a result of the radial beryllium reflectors.

4.2 REACTIVITY COEFFICIENTS.

Reactivity Coefficients were calculated from the MCNP5 output. Graphs of reactivity with moderator temperature, fuel temperature and void were plotted and presented in figures 4.6 to 4.8.

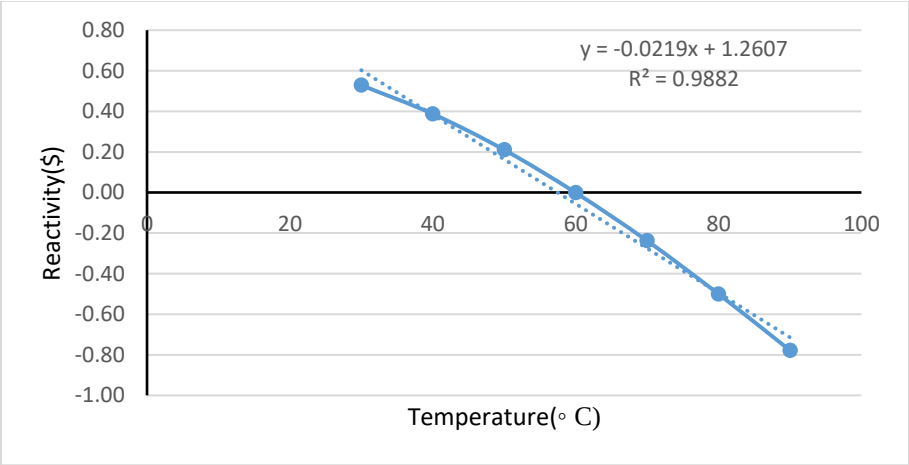

Figure 4.6: Moderator Temperature against Reactivity.

The reactivity coefficients were used in the PARET code to simulate transient conditions. From figure 4.6, the moderator temperature reactivity feedback has a negative gradient of -0.0219. The reactivity response to change in temperature is linear .The graph shows a regression of 0.9882 which is fairly close to unity thus showing a good fit for the data. This shows a strong correlation for the two parameters, Moderator Temperature and Reactivity. Figure 4.7 also presents a graph of the moderator void and temperature. The response is nearly linear and the regression of the graph indicates a good fit of the data points.

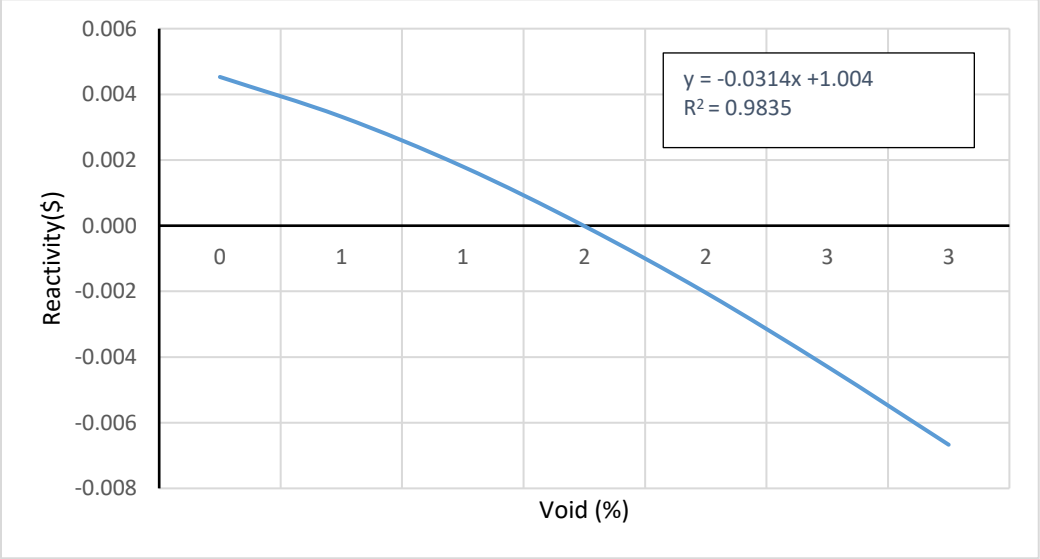

Figure 4.7: Void Temperature feedback.

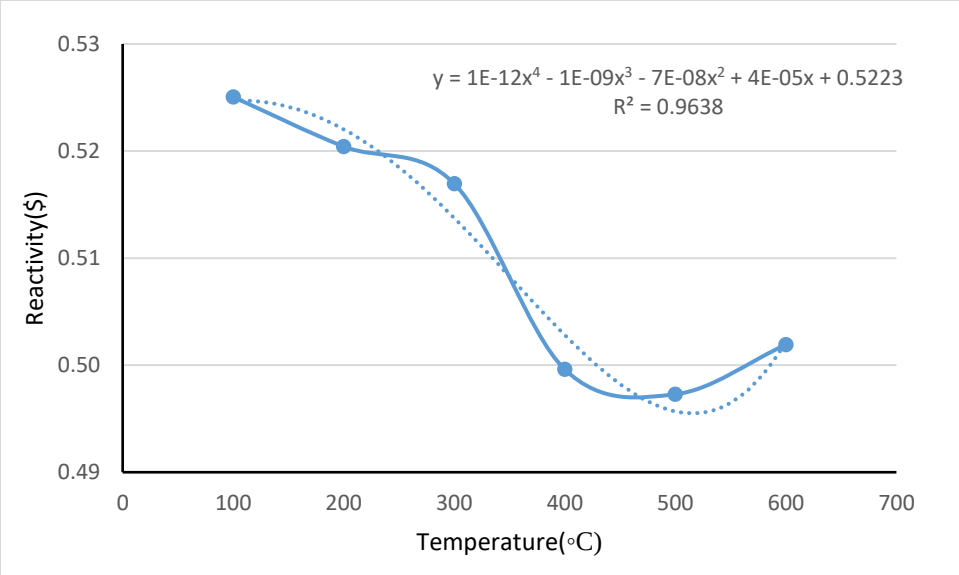

Figure 4.8: Reactivity feedback for Fuel Temperature.

Figure 4.8 shows the relationship between reactivity and fuel temperature, a non-linear relationship was observed for a graph of fuel temperature and reactivity. This is credited to the resonance behavior of the fuel temperature cross section. A regression of 0.9638 was computed which indicates a strong fit between data points. The reactivity coefficient was determined using the fourth order differential equation obtained from the graph.

4.3 Transient Analysis

Figure 4.9 represents the reactor power response to reactivity insertions of 1.94 mk, 2.1 mk, 2.99 mk, 3.87 mk, 4.0 mk and 6.71 mk. From figure 4.9, from an initial low power of 2 W, the power begins to increase after about 100 s and peaks 120 s of reactivity insertion and starts to decline in power after about 350 s to 500 s. A high peak power of 193.34 kW is recorded for a reactivity insertion of 6.71 mk and a relatively low peak of 30.24 kW is recorded for reactivity insertion of 1.94 mk.

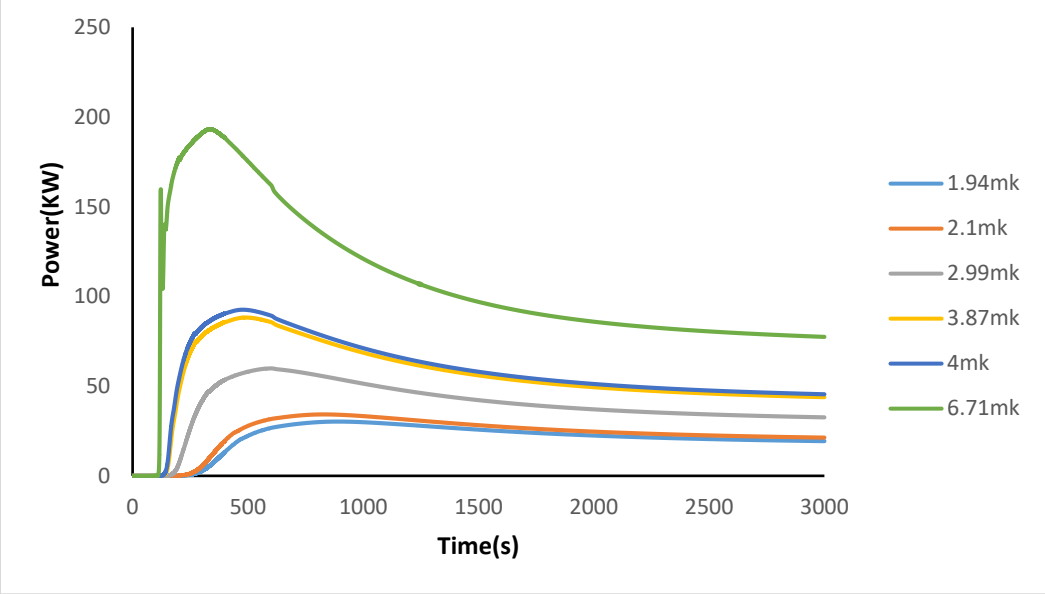

Figure 4.9: Peak Power for varying reactivity insertions.

It is observed from figure 4.9 above that for high excess reactivity insertion the power increases sharply within 120 seconds of the reactivity insertion, but for lower reactivity insertions, there is a gradual rise in power. A quick rise in power is observed for the 6.71 mk reactivity insertion which reaches its maximum power of 193.3 kW in 341 s. For reactivity insertions of 2.99 mk and 4.0 mk, the maximum power of 59.89 kW and 92.60 kW was reached at 602 s and 477 s respectively.

The peak power for an insertion of 2.1 mk was found to be 34.234 kW which compares well with the nominal power of the LEU core. Comparing this to a fresh core insertion of 4mk, the power peaks to a power of 92.60 kW which is 2.7 times the nominal power of the core. The figure 4.9 on peak power demonstrates the inherent safety in the GHARR-1 with LEU core owing to a negative temperature coefficient which helps in stabilizing the reactor during a ramp reactivity insertion, thus decreasing the power after peaking.

The response of the coolant in the LEU core of GHARR-1 under various reactivity insertions are illustrated in figures 4.10.

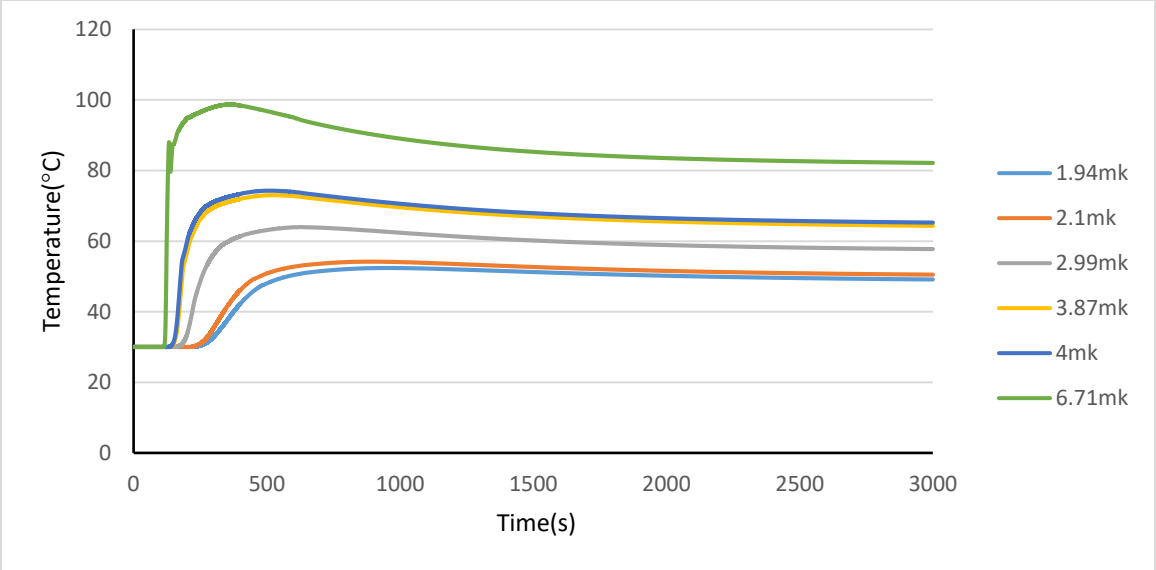

Figure 4.10: Comparison of Coolant Temperatures for varying reactivity insertions.

From Figure 4.10, a maximum coolant temperature of 98 ˚C is recorded for a reactivity insertion of 6.71 mk. Although this temperature is below the boiling point of water, (100 ˚C), it is closer and ineffective cooling and moderation of neutrons alongside flow instabilities may occur in the core at such temperatures. Nonetheless, boiling of the coolant is not envisaged in the core. All other reactivity insertions have coolant temperatures relatively far below the boiling point of water.

The clad temperatures for various reactivity insertions are presented in figure 4.11. The maximum clad temperature of 133.45 ˚C was recorded for a ramp reactivity insertion of 6.71 mk. This value is far below the melting point of the zircaloy -4 cladding which is 1850 ˚C and hence the clad will be able to withstand such conditions without a compromise in its mechanical properties.

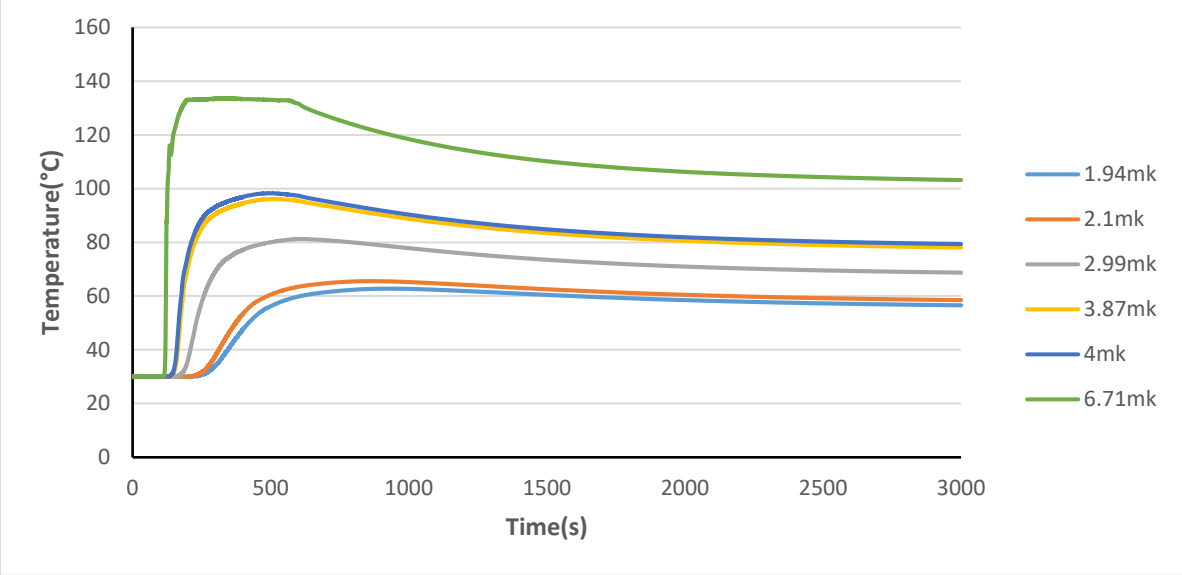

Figure 4.11: Comparison of Clad Temperatures for varying reactivity insertions.

The melting point of UO_2 is 2800 ˚C, for the various reactivity insertions simulated, the maximum temperature within the fuel pellet was found to be far below the melting point of the fuel and hence the fuel structural integrity will be maintained even at such accident scenarios. The fuel temperature rose to 137 ˚C for a 6.71 mk ramp reactivity insertion.

A 15.35 ˚C change in fuel temperature was recorded when the reactivity insertion was varied from 2.99 mk to 3.87 mk. Figure 4.12 shows the relationship between the fuel center line temperatures for various reactivity insertions.

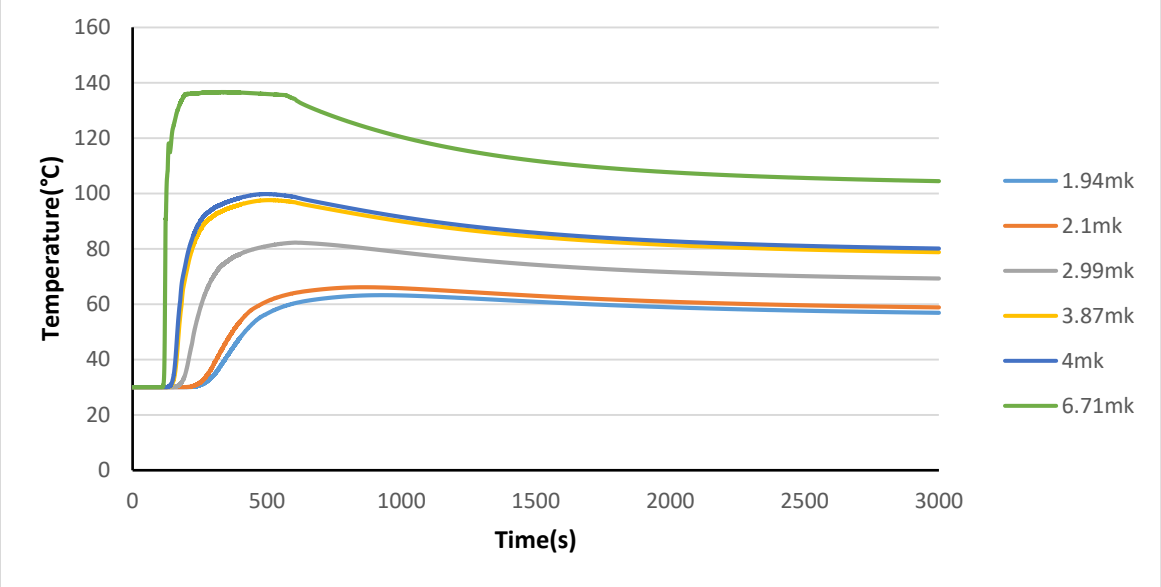

Figure 4.12: Comparison of fuel Centre line Temperatures for varying reactivity insertions.

Change in temperatures between the fuel, clad and coolant for ramp insertions of reactivity are presented in the figures 4.13 to 4.18. It was observed that the change in temperature between fuel and clad was relatively low within the range of 0.50˚C to 3.18˚C. This demonstrates the effective transfer of heat from the UO_2 fuel to the Zircaloy-4 clad. Hence there will not be excessive build-up of heat in the fuel since almost all the heat generated will be transferred to the coolant through the clad.

A change in temperature range of 10.36 ˚C to 34.70 ˚C between the clad and coolant for reactivity insertions of 1.94 mk to 6.7 1 mk was observed, that is, heat transfer between the clad and coolant increases with reactivity insertion.

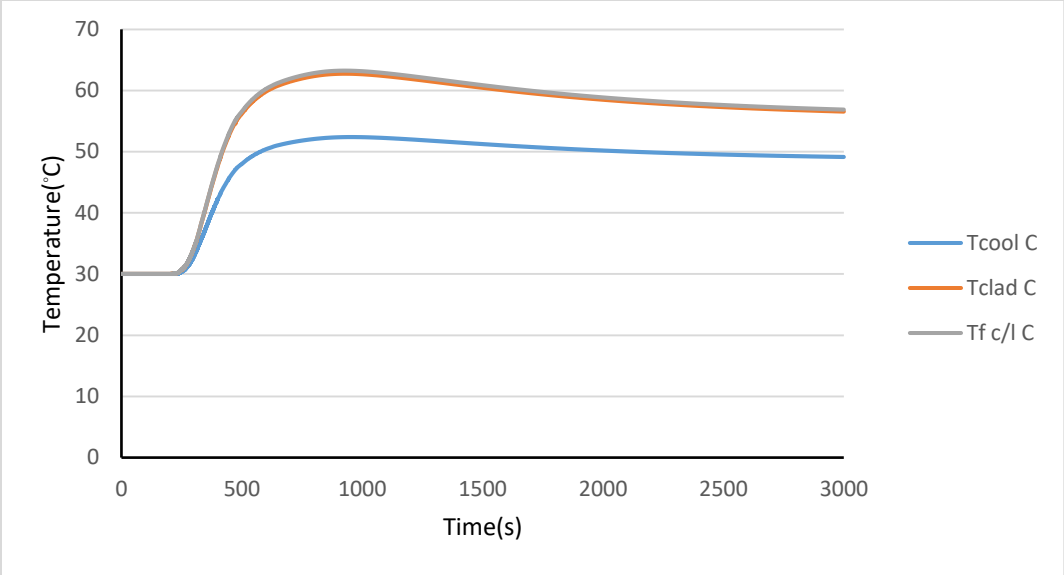

Figure 4.13: Temperature variations for 1.94 mk insertion.

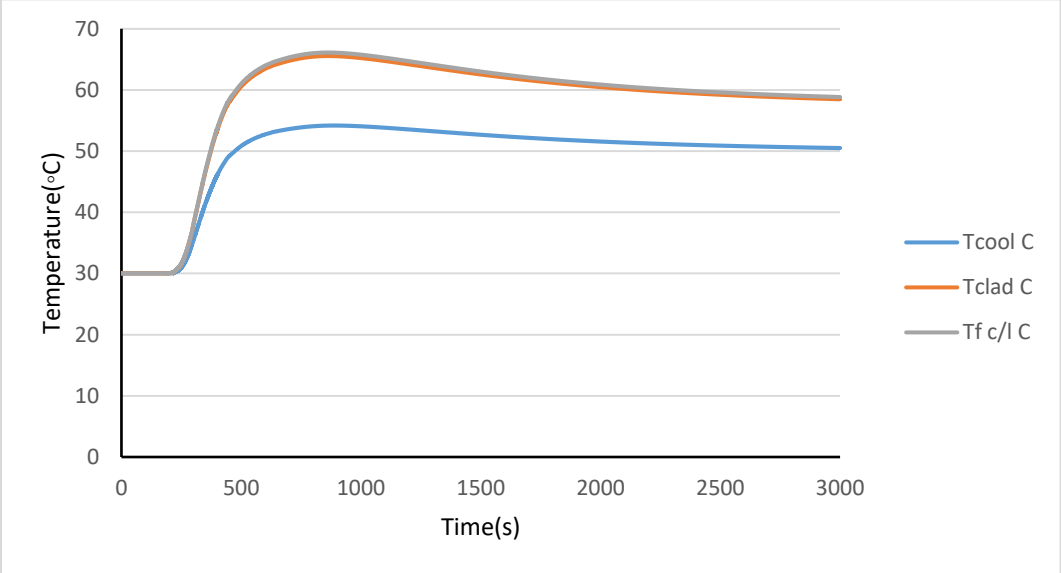

Figure 4.14: Temperature variations for 2.1 mk insertion.

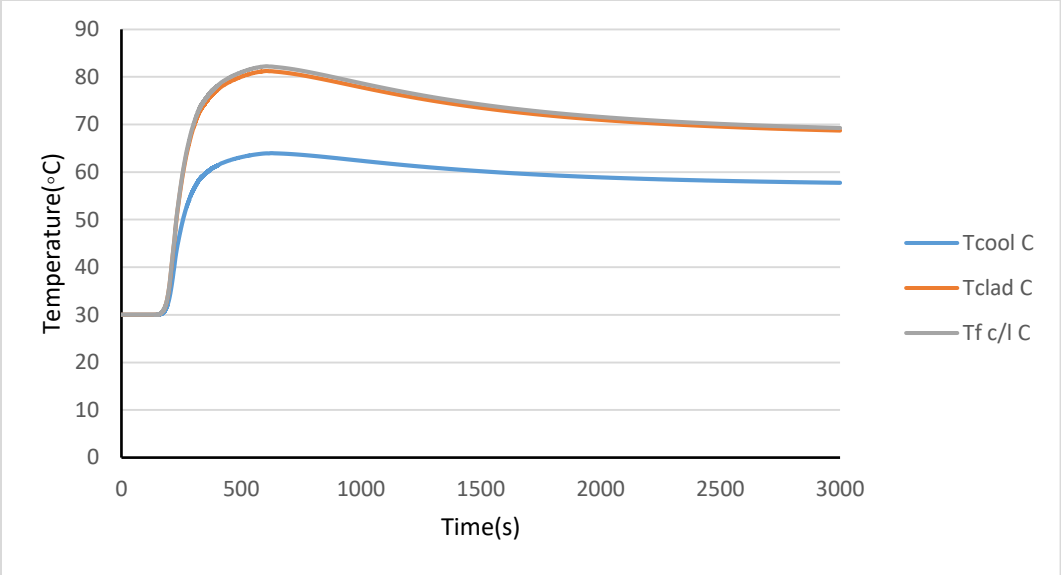

Figure 4.15: Temperature variations for 2.99 mk insertion.

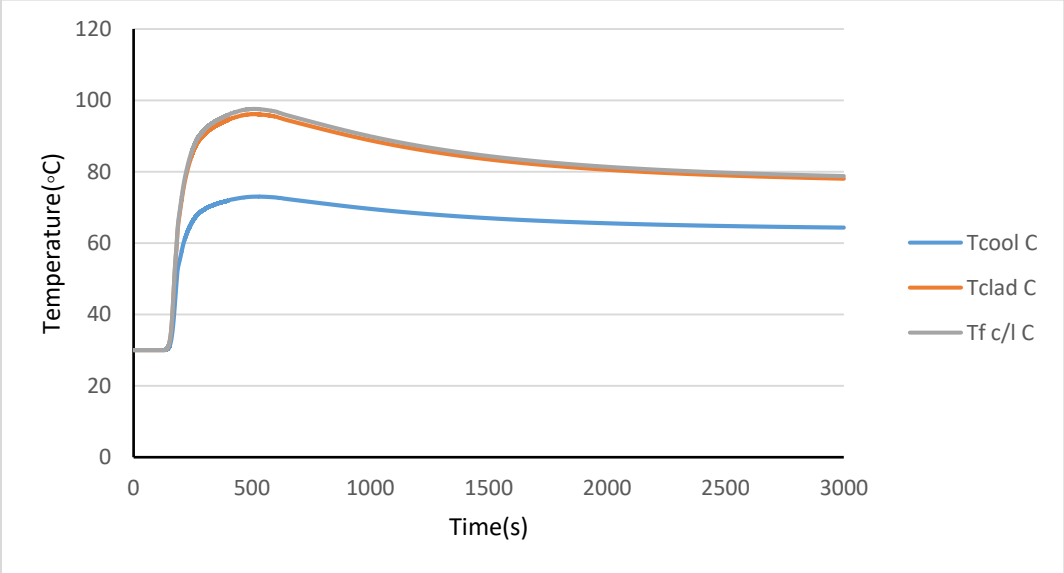

Figure 4.16: Temperature variations for 3.87 mk insertion.

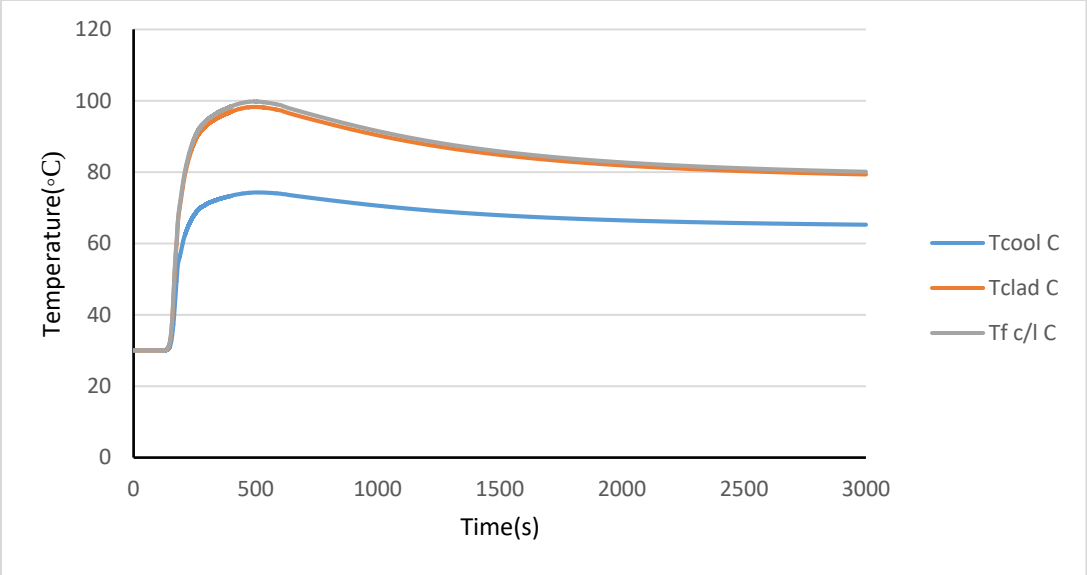

Figure 4.17: Temperature variations for 4.0 mk insertion.

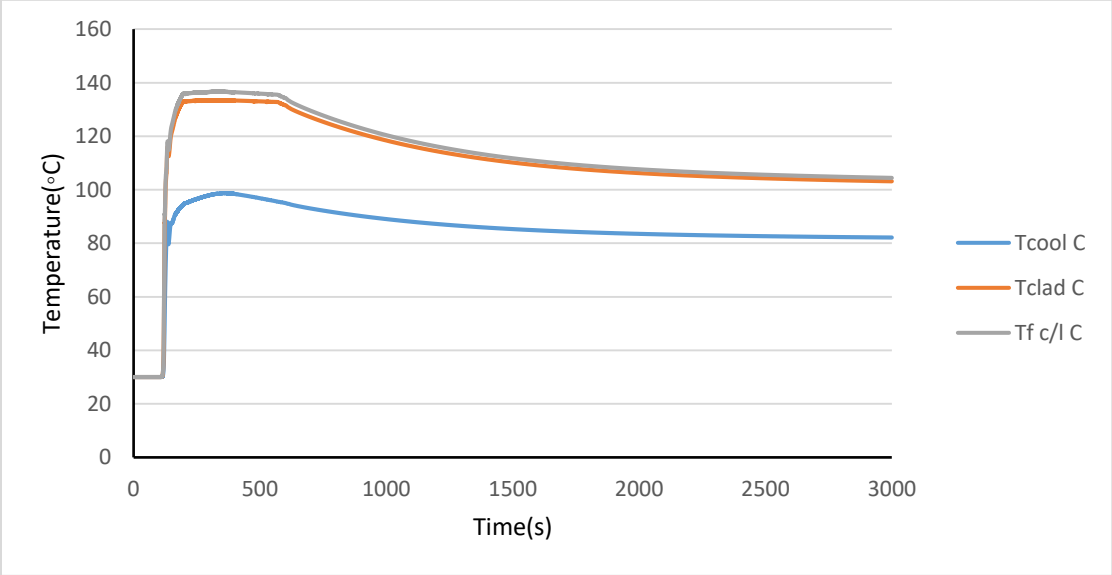

Figure 4.1: Temperature variations for 6.71 mk insertion.

4.4 Comparison of PARET output with experimental data.

The data obtained from this work was validated by comparing the outputs of the PARET run with experimental data on GHARR-1 with LEU core after the core conversion.

From experiments conducted for clean core ramp insertion of 3.87 mk and 2.99 mk insertion of GHARR-1 with LEU core, the data obtained was compared with the results from the PARET run. The peak power and outlet coolant temperatures for 2.99 mk and 3.87 mk reactivity insertions are compared in figures 4.19 and 4.20.

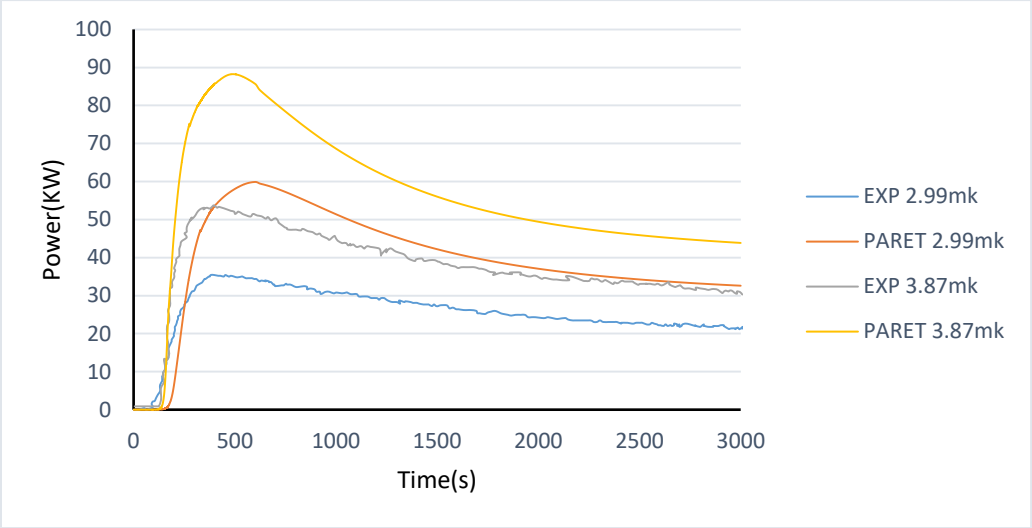

Figure 4.19: Comparison of power profile for PARET and Experimental data of GHARR-1 LEU core.

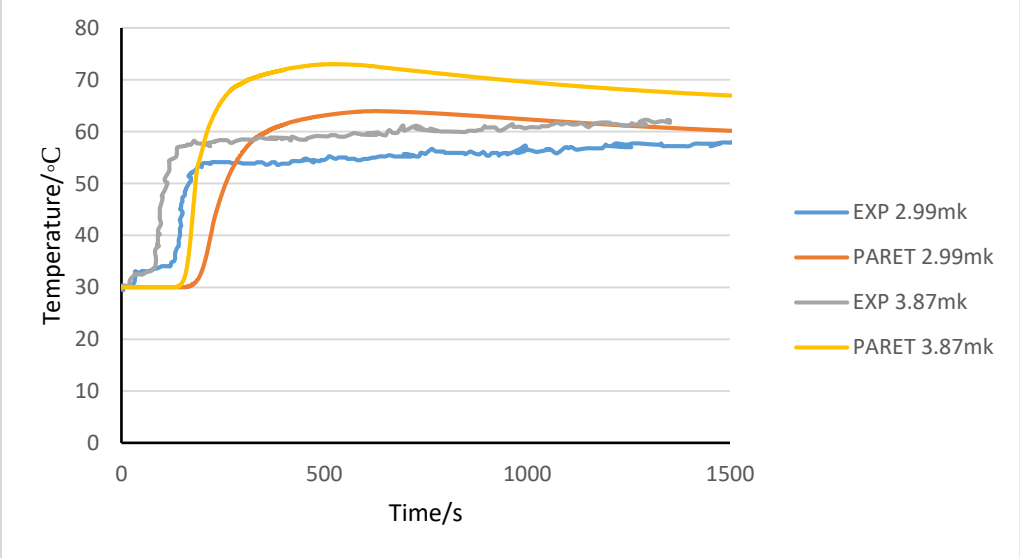

Figure 4.20: Comparison of Coolant temperature for PARET and Experimental data of GHARR-1 LEU core.

From figures 4.19 and 4.20, the peak powers of 59.89 kW and 88.23 kW for 2.99 mk and 3.87 mk reactivity insertions were obtained from the PARET run which compared well with peak powers of 35.42 kW and 53.74 kW obtained experimentally for 2.99 mk and 3.87 mk respectively. For 2.99 mk and 3.87 mk, PARET run outlet coolant temperatures of 60.11 °C and 67.38 °C correlated well with the experimentally obtained outlet coolant temperatures of 59.09 °C and 62.30 °C from reactivity insertions of 2.99 mk and 3.87 mk respectively.

4.5 Comparison of PARET output for LEU and HEU Cores.

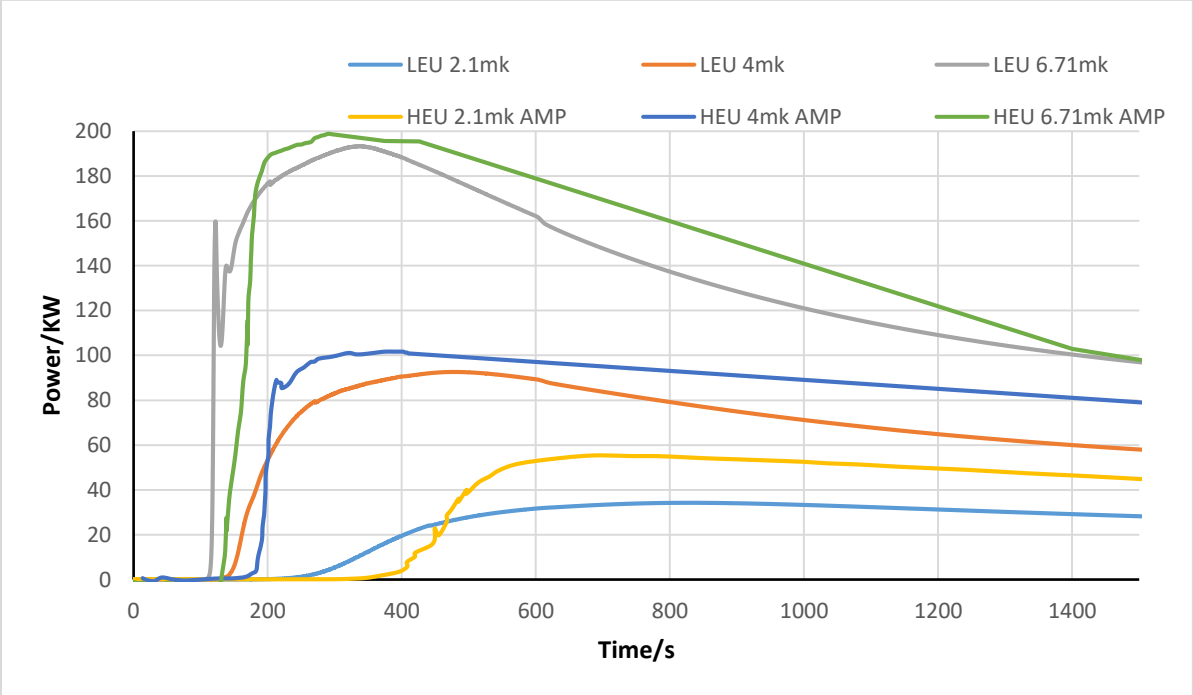

Figure 4.21 : Comparison of power profile for HEU and LEU PARET run.

The peak power for GHARR with LEU core under various reactivity insertions was compared with data for the former HEU core obtained from literature[4] (figure 4.21). For a clean core insertion of 4 mk, a peak power of 94.78 kW was obtained for the LEU which compared well with a peak power of 102.78 kW for the former HEU core. For accident conditions, that is an insertion of 6.71 mk, a peak power of 192.23 kW and 189.87 kW was recorded for LEU and HEU cores respectively.

4.6 Steady state thermal hydraulic analysis

Steady state simulations were run for the nominal LEU core power of 34 kW and other operable powers: 30 kW, 17 kW and 15 kW. Computed Values for the FIR, DNBR and ONBR are shown in Table 4.1 below. It can be observed that the three safety margins, ONBR, DNBR and FIR decreases with the increase of reactor power. Thus the higher these safety margins the safer the reactor is at the nominal reactor power. ONBR is the ratio of power at the ONB to the nominal power. DNBR is the ratio of power corresponding to the critical heat flux to the nominal power corresponding to the actual heat flux. FIR is the ratio of power at the onset of flow instability to the nominal power[11], [30], [65]. The computed values of the ONBR and the DNBR indicates there will be no boiling crisis in the core at the nominal power. The criteria of thermal-hydraulic design for GHARR-1 MNSR require that the DNBR should be greater than 2.55 [66], [67]. The values obtained are within the limits of safety for the operating power of the LEU core. The values obtained for the computations of the coolant and clad surface temperatures using 30 °C as the inlet temperature and 1 bar as coolant pressure are also represented in Table 4.1.

Table 4.1: Steady state thermal hydraulic analysis of GHARR-1 with LEU core.

Parameter/Power	**15KW**	**17KW**	**30KW**	**34KW**
Core flow rate (Kg/s)	0.293	0.307	0.378	0.397
Coolant Temperature(˚C)	43.77	44.90	51.28	53.01
Maximum Clad Temperature(˚C)	80.47	85.05	111.98	120.30
Peak Fuel Temperature(˚C)	80.63	85.23	112.28	120.64
ONBR	1.65	1.51	1.27	1.12
FIR	5.69	5.24	3.58	3.19
DNBR	14.27	13.82	7.22	6.84

The results also indicates good safety margins for operation of GHARR 1 with LEU core since the peak temperatures for the clad and the fuel were found to be far below the melting point of the zircaloy -4 clad(1850 ˚C) and UO_2 fuel (2850 ˚C). The change in temperature from the fuel to the clad was found to be in the range of 0.152 ˚C to 0.346 ˚C indicating an effective conductivity of heat from the fuel meat to the clad.

Table 4.2: Comparison of outlet coolant temperatures using PLTEMP and experimental data.

Inlet Coolant Temperature(˚C)	Outlet Coolant Temperature (˚C). PLTEMP	Outlet Coolant Temperature (˚C). EXPERIMENT
Power =17 kW		
38.50	50.73	51.0
40.70	54.15	53.2
41.90	54.68	54.1
42.40	54.53	54.4
43.50	56.57	56.3
Power =34 kW		
35.30	55.89	54.5
37.40	59.08	56.6
39.10	60.48	57.8
41.50	61.72	59.4
44.50	65.16	62.2

Table 4.2 shows comparison for the outlet coolant temperatures of the steady state simulation using PLTEMP and experimental data at half nominal power (17 kW) and full nominal power (34 kW). The outlet coolant temperatures compared well with the experimental values. A deviation in the range of 0.48% to 4.76% from the experimental values is observed. This indicates a good reliance on the data obtained from the simulation.

Table 4.3:Comparison of PLTEMP output for HEU and LEU core of GHARR-1.

Parameter	**15KW**		**30KW**		**34KW**	
Power	**HEU**	**LEU**	**HEU**	**LEU**	**HEU**	**LEU**
Core flow rate (Kg/s)	0.2948	0.2930	0.3804	0.3783	0.3986	0.3965
Maximum Coolant Temperature(˚C)	42.995	43.766	50.103	51.280	51.739	53.013
Maximum Clad Temperature(˚C)	78.245	80.474	107.736	111.978	115.487	120.297
Peak Fuel Temperature(˚C)	78.370	80.626	107.986	112.282	115.770	120.643

Table 4.3 shows a comparison of the results obtained from the PLTEMP simulation of GHARR-1 with LEU and previous HEU core. There is no significant difference in change in temperature from the fuel meat to the clad for both LEU and HEU cores. The temperature drop in LEU was in the range of 0.152 ˚C to 0.346 ˚C as compared to 0.125 ˚C to 0.283 ˚C in the HEU. These variations could be accredited to the variation in fuel composition and material change of the clad. The results show that under steady state and normal operating conditions of the reactor, the fuel meat, clad and coolant temperatures obtained are slightly higher in the LEU core than that of the HEU core. This finding is contrary to that obtained under reactor transient conditions, where the obtained temperatures for fuel meat, clad and coolant are higher in the HEU core than that in the LEU core.

CHAPTER 5

5. CONCLUSION AND RECOMMENDATION

5.1 CONCLUSION

Thermal hydraulic analysis of Ghana Research Reactor-1 with low enriched uranium core has been studied. Reactor core neutronic values were obtained by modelling the core using MCNP5, transient and steady state thermal hydraulic analysis were studied using the PARET/ANL and PLTEMP/ANL. The behaviour of the reactor core at normal and accident conditions of large reactivity insertions were studied. Transient results obtained for accidental large reactivity insertions of 6.71 mk indicated that boiling might occur in the coolant because, under such large reactivity insertions, the coolant temperature was close to the saturation temperature of the coolant. Steady state results also indicate good safety margins for operation of GHARR 1 with LEU core since the peak temperatures for the clad and the fuel were found to be far below the melting point of the zircaloy -4 clad (1850 ˚C) and UO_2 fuel (2850 ˚C). Hence the integrity of the fuel material and clad will not be compromised under accident scenarios of large reactivity insertions. The data obtained compared well with experimental data available. Comparison of results with previous HEU core has shown that temperature rise in the LEU core is lower than that in the HEU core under reactor transient conditions, whereas under steady state and normal operating conditions the temperature rise in the LEU core is slightly higher than that in the HEU core. Also, the reactor is inherently safe even at accident conditions.

5.2 RECOMMENDATIONS

Further studies on the current LEU core in the field of thermal hydraulic analysis is recommended in the following;

- A study on the heat transfer and analysis of the new LEU core of GHARR-1 at shutdown be investigated to consider the quantum of decay heat produced and its removal from the core.

- A study on reactor noise of the new LEU core of GHARR-1 to ascertain the perturbations in the core.
- A CFD code be used to investigate the heat transfer and distribution in the core sub channels of GHARR-1 with LEU.

REFERENCES

[1] L. A. Khan, I. H. Bokhari, K. M. Akhtar, and S. Pervez, "Steady State Thermal Hydraulic Analysis of Leu," no. PINSTECH-122, p. 51, 1991.

[2] M. Siman-Tov, W. R. Gambill, W. R. Nelson, A. E. Ruggles, and G. L. Yoder, "Thermal-hydraulic correlations for the advanced neutron source reactor fuel element design and analysis," in *American Society of Mechanical Engineers, Heat Transfer Division, (Publication) HTD*, 1991, vol. 190.

[3] R. Pericas, K. Ivanov, F. Reventós, and L. Batet, "Code improvement and model validation for Ascó-II Nuclear Power Plant model using a coupled 3D neutron kinetics/thermal-hydraulic code," *Ann. Nucl. Energy*, vol. 87, pp. 366–374, 2016.

[4] E. Ampomah-Amoako, E. H. K. Akaho, S. Anim-Sampong, and B. J. B. Nyarko, "Transient analysis of Ghana Research Reactor-1 using PARET/ANL thermal-hydraulic code," *Nucl. Eng. Des.*, vol. 239, no. 11, pp. 2479–2483, 2009.

[5] S. Yamoah, E. H. K. Akaho, B. J. B. Nyarko, M. Asamoah, A. G. Ampong, and E. O. Amponsah-Abu, "Analysis of thermal-hydraulic transients for the Miniature Neutron Source Reactor (MNSR) in Ghana," *Res. J. Appl. Sci. Eng. Technol.*, vol. 3, no. 8, pp. 737–745, 2011.

[6] S. Jewer, A. G. Buchan, C. C. Pain, and D. G. Cacuci, "An immersed body method for coupled neutron transport and thermal hydraulic simulations of PWR assemblies," *Ann. Nucl. Energy*, vol. 68, pp. 124–135, 2014.

[7] D. Springfels, K. A. Jordan, and D. Schubring, "Comparison of thermal

hydraulic analysis methods (CODES) for the university of Florida training reactor (UFTR)," *Int. Top. Meet. Nucl. React. Therm. Hydraul. 2015, NURETH 2015*, 2015.

[8] E. H. K. Akaho and B. J. B. Nyarko, "Characterization of neutron flux spectra in irradiation sites of MNSR reactor using the Westcott-formalism for the k0neutron activation analysis method," *Appl. Radiat. Isot.*, vol. 57, no. 2, pp. 265–273, 2002.

[9] E. E. Lewis, "Fundamentals of Nuclear Reactor Physics," *Elsevier*, p. 280, 2008.

[10] A. Salawu and G. I. Balogun, "Prediction of Peak Temperatures of Nigeria Research Reactor Core Components under Several Reactivity Accident Tests ," vol. 2, no. 1, pp. 67–71, 2017.

[11] IAEA, "Safety of Research Reactors," *Specif. Saf. Requir. No. SSR-3*, 2016.

[12] W. M. Stacey, "Nuclear Reactor Dynamics," in *Nuclear Reactor Physics*, 2007, pp. 143–195.

[13] U. Doe, "Doe handBook 1019/1-93 nuclear physics and reactor theory," *Nucl. Phys.*, vol. 1, no. January, pp. 2238–2239, 1993.

[14] Lamarsh JR, "Introduction to Nuclear Reactor Theory," *Interactions*, vol. 9, no. Spring, pp. 1–5, 2005.

[15] R. Madi, "Analysis Of Doppler Reactivity Coefficient On The Typical Pwr-1000 Reactor With Mox Fuel," *KnE Energy*, vol. 1, no. 1, pp. 1–9, 2016.

[16] A. W. Solbrig, "Doppler Effect in Neutron Absorption Resonances," *Am. J. Phys.*, vol. 29, no. 4, pp. 257–261, 1961.

[17] R. Barati and S. Setayeshi, "A model for nuclear research reactor dynamics," *Nucl. Eng. Des.*, vol. 262, pp. 251–263, 2013.

[18] S. Dawahra, K. Khattab, and G. Saba, "Reactivity temperature coefficients for the HEU and LEU fuel of the MNSR reactor," *Prog. Nucl. Energy*, vol. 88, pp. 28–32, Apr. 2016.

[19] US Department of Energy, "Thermodynamics , Heat Transfer , And Fluid Flow , DOE Fundamentals Handbook," *Energy*, vol. 1, p. 138, 1992.

[20] S. A. Agbo, Y. A. Ahmed, I. O. B. Ewa, and Y. Jibrin, "Analysis of Nigeria Research Reactor-1 Thermal Power Calibration Methods," *Nucl. Eng. Technol.*, vol. 48, no. 3, pp. 673–683, 2016.

[21] S. Holm, "Nuclear reactor theory," *Nucl. Phys.*, vol. 10, p. 627, 1959.

[22] G. Chen, "Ballistic-diffusive heat-conduction equations," *Phys. Rev. Lett.*, vol. 86, no. 11, pp. 2297–2300, 2001.

[23] Y. Abbassi, S. Asgarian, E. Ghahremani, and M. Abbasi, "Investigation of natural convection in Miniature Neutron Source Reactor of Isfahan by applying the porous media approach," *Nucl. Eng. Des.*, vol. 309, pp. 213–223, 2016.

[24] A. K. Sharma and C. Balaji, "A numerical study of natural convection from a localized heat source in the lower plenum of a fast breeder reactor under failed conditions," *Heat Mass Transf. und Stoffuebertragung*, vol. 40, no. 11, pp. 853–858, 2004.

[25] Abrefah,R. G., "Neutronics And Dose Calculation For Prospective Spent Nuclear Fuel Cask For Gharr-1 Facility,"*A PhD dissertation submitted to the University of Ghana* , 2014.

[26] D. L. Feldman, "Using planning scenarios for DOE radioactive waste management: The case of the Advanced Neutron Source," in *High Level Radioactive Waste Management - Proceedings of the Annual International Conference*, 1994, vol. 3.

[27] J. Jiang, B. Yuan, J. Zou, and Y. Wu, "Activation analysis and waste management for blanket materials of multi-functional experimental fusion-fission hybrid reactor (FDS-MFX)," *Fusion Eng. Des.*, vol. 89, no. 4, pp. 405–411, 2014.

[28] K. Inoue, N. Otomo, H. Iwasa, and Y. Kiyanagi, "Slow neutron spectra in cold moderators," *J. Nucl. Sci. Technol.*, vol. 11, no. 5, pp. 228–229, 1974.

[29] E. Zarifi, S. Tashakor, and J. Khorsandi, "Steady state and transient analyses of MNSR reactor using RELAP5 code," *Kerntechnik*, vol. 81, no. 1, pp. 25–33, 2016.

[30] Hainoun, A., Doval, A., Umbehaun, P., Chatzidakis, S., Ghazi, N., Park, S., Mladin, M. and Shokr, A., "International benchmark study of advanced thermal hydraulic safety analysis codes against measurements on IEA-R1 research reactor," *Nucl. Eng. Des.*, vol. 280, no. June, pp. 233–250, 2014.

[31] Buchan, A. G., Pain, C. C., Goddard, A., J H Eaton, M. D., Gomes, J., L M A Gorman, G. J., Cooling, C. M., Tollit, B. S., Nygaard, E. T., Glenn, D. E. and Angelo, P. L., "Simulated transient dynamics and heat transfer characteristics of the water boiler nuclear reactor - SUPO - with cooling coil heat extraction," *Ann. Nucl. Energy*, vol. 48, pp. 68–83, 2012.

[32] E. H. K. Akaho and B. T. Maakuu, "Simulation of reactivity transients in a miniature neutron source reactor core," *Nucl. Eng. Des.*, vol. 213, no. 1, pp. 31–42, 2002.

[33] S. A. Jonah, K. Ibikunle, and Y. Li, "A feasibility study of LEU enrichment uranium fuels for MNSR conversion using MCNP," *Ann. Nucl. Energy*, vol. 36, no. 8, pp. 1285–1286, 2009.

[34] IAEA, “Management of high enriched uranium for peaceful purposes: Status and trends,” *Iaea-Tecdoc-1452*, no. June, 2005.

[35] Argonne Natiional Laboratory(ANL) J. R. R. Program and Nuclear. Engineering Division, “MNSR flux performance and core lifetime analysis with HEU and LEU fuels,” 2008.

[36] F. D’Auria, "Thermal-Hydraulics of water cooled nuclear reactors". *woodhead publishing*, 2017.

[37] P. Savva, M. Varvayanni, A. C. Fernandes, J. G. Marques, and N. Catsaros, “Comparing neutronics codes performance in analyzing a fresh-fuelled research reactor core,” *Ann. Nucl. Energy*, vol. 63, pp. 731–741, 2014.

[38] E. L. Redmond and J. M. Ryskamp, “Monte-Carlo Methods, Models, and Applications to the Advanced Neutron Source,” *Nucl. Technol.*, vol. 95, no. 3, pp. 272–286, 1991.

[39] E. K. Boafo, E. Alhassan, and E. H. K. Akaho, “Utilizing the burnup capability in MCNPX to perform depletion analysis of an MNSR fuel,” *Ann. Nucl. Energy*, vol. 73, pp. 478–483, 2014.

[40] M. Adorni, A. Bousbia-salah, F. D’Auria, and T. Hamidouche, “Accident analysis in research reactors,” *Nucl. Energy New Eur. Int. Conf.*, p. 202.1-202.9, 2007.

[41] A. Petruzzi and F. D’Auria, “Thermal-Hydraulic System Codes in Nulcear Reactor Safety and Qualification Procedures,” *Sci. Technol. Nucl. Install.*, vol. 2008, no. vi, pp. 1–16, 2008.

[42] Obenchain C.F, “PARET-A Program for the Analysis of Reactor Transients”,” *IDO-17282*, 1969.

[43] W. L. Woodruff, “A Kinetics and Thermal-Hydraulics Capability for the Analysis of Research Reactors,” *Nucl. Technol.*, vol. 64, no. 2, pp.

196–206, 2017.

[44] Adoo, N. A., Nyarko, B. J.B., Akaho, E. H.K., Alhassan, E., Agbodemegbe, V. Y., Bansah, and C. Y., Della, R. "Determination of thermal hydraulic data of GHARR-1 under reactivity insertion transients using the PARET/ANL code," *Nucl. Eng. Des.*, vol. 241, no. 12, pp. 5203–5210, 2011.

[45] S. A. Jonah, Y. V. Ibrahim, A. S. Ajuji, and M. Y. Onimisi, "The impact of HEU to LEU conversion of commercial MNSR: Determination of neutron spectrum parameters in irradiation channels of NIRR-1 using MCNP code," *Ann. Nucl. Energy*, vol. 39, no. 1, pp. 15–17, 2012.

[46] I. H. Bokhari and S. Pervez, "Safety analysis for core conversion (from HEU to LEU) of Pakistan research reactor-2 (PARR-2)," *Nucl. Eng. Des.*, vol. 240, no. 1, pp. 123–128, 2010.

[47] H. C. Odoi, "Reactor Core Conversion Studies of Ghana Research Reactor – 1 and Proposal for Addition of Safety Rod," *Diss. Submitt. to Univ. Ghana*, vol. 2004, no. June, 2014.

[48] Odoi, H.C., Akaho, E.H.K., Jonah, S.A., Abrefah, R.G., Ibrahim, V.Y., "Study of Criticality Safety and Neutronic Performance for a 348-Fuel-Pin Ghana Research Reactor-1 LEU Core Using MCNP Code.," *World J. Nucl. Sci. Technol.*, vol. 4, pp. 46–52, 2014.

[49] W. Woodruff and R. Smith, "A users guide for the ANL version of the PARET code, PARET/ANL .," *local Threat Reduct. Initiat. – Convers. Progr. Nucl. Eng. Div. Argonne*, vol. TM 16, 2007.

[50] B. M. Mweetwa, E. Ampomah-amoako, E. Horga, K. Akaho, and C. Odoi, "Prediction of Neutronic and Kinetic Parameters of Ghana Research Reactor 1 (GHARR-1) after 19 Years of Operation Using Monte Carlo-N Particle (MCNP) Code," pp. 160–175, 2018.

[51] H. C. Odoi, E. H. K. Akaho, B. J. B. Nyarko, and R. G. Abrefah, 2014. "Current Studies of Conversion of Ghana Research Reactor Core to Low Enriched Uranium." Technical Report, Ghana Atomic Energy Commision.

[52] Jonah S.A., Ibrahim,V.Y., Kalimullah,M. and Matos, J.E., Steady state thermal hydraulic operational parameters and safety margins of NIRR-1 with LEU fuel using PLTEMP/ANL. *ENC 2012 Transactions-Research Reactors*, 2012, pp. 5–12.

[53] Ž. Štancar, L. Barbot, C. Destouches, D. Fourmentel, J. F. Villard, and L. Snoj, "Computational validation of the fission rate distribution experimental benchmark at the JSI TRIGA Mark II research reactor using the Monte Carlo method," *Ann. Nucl. Energy*, vol. 112, pp. 94–108, 2018.

[54] J. K. Shultis and R. E. Faw, "An MCNP Primer," *Structure*, vol. 66506, no. c, pp. 0–45, 2006.

[55] J. Kestin, J. V. Sengers, B. Kamgar-Parsi, and J. M. H. Levelt Sengers, "Thermophysical Properties of Fluid H2O," *J. Phys. Chem. Ref. Data*, vol. 13, no. 1, pp. 175–183, 1984.

[56] National Institute of Standards and Technology, "Isobaric Properties for Water." pp. 1–15, 2016.

[57] M. M. Bretscher, "Evaluation of reactor kinetic parameters without the need for perturbation codes," *Int. Meet. Reduc. Enrich. …*, 1997.

[58] F. Ameyaw, A. Ayensu, and E. H. K. Akaho, "Modeling and simulation of coupled nuclear heat energy deposition and transfer in the fuel assembly of the Ghana Research Reactor-1 (GHARR-1)," *Nucl. Eng. Des.*, vol. 241, no. 12, pp. 5183–5188, Dec. 2011.

[59] R. G. Abrefah, B. J. B. Nyarko, E. H. K. Akaho, S. Anim Sampong, and

R. B. M. Sogbadji, “Axial and radial distribution of thermal and epithermal neutron fluxes in irradiation channels of the Ghana research reactor-1 using foil activation analysis,” *Ann. Nucl. Energy*, vol. 37, no. 8, pp. 1027–1035, 2010.

[60] A. K. Nayak, P. K. Vijayan, D. Saha, V. V. Raj, and M. Aritomi, “Study on the stability behaviour of a natural circulation pressure tube type boiling water reactor,” *Nucl. Eng. Des.*, vol. 215, no. 1–2, pp. 127–137, 2002.

[61] S. Lepri, R. Livi, and A. Politi, “Heat conduction in chains of nonlinear oscillators,” *Phys. Rev. Lett.*, vol. 78, no. 10, pp. 1896–1899, 1997.

[62] N. E. Division, “Comparison of the PLTEMP Code Flow Instability Predictions with Measurements Made with Electrically Heated Channels for the Advanced Test Reactor”, ANL/RERTR/TM-11-23, June 9, 2011.

[63] M. M. Rahman, M. A. R. Akond, M. K. Basher, and Q. Huda, “Steady-State Thermal-Hydraulic Analysis of TRIGA Research Reactor,” *World J. Nucl. Sci. Technol.*, vol. 4, no. April, pp. 81–87, 2014.

[64] A. P. Olson, S. A. Jonah, and R. Program, “MNSR transient analyses and thermal-hydraulic safety margins for HEU and LEU cores using PARET" , *Centre for Energy Research and Training*,” pp. 1–13.

[65] H. Omar, N. Ghazi, and A. Hainoun, “Thermal hydraulic and safety analysis for core conversion (HEU-LEU) of Syrian Miniature Neutron Source Reactor,” *Prog. Nucl. Energy*, 2012.

[66] Shitsi, E., Akaho, E.H.K., Nyarko, B.J.B., “Theoretical investigations of two-phase flow and heat transfer in parallel multichannel core of a low power reactor,” *Issues Sci. Res.*, vol. 2, no. 1, pp. 1–17, 2018.

[67] Akaho, E.H.K., Anim-Sampong, S., Dodoo-Amoo, D.N.A., Maakuu,

B.T., Emi-Reynolds, G., Osae, E.K., Boadu, H.O., Bamford, “Ghana Research Reactor-1 Final Safety Analysis Report.,” *Ghana At. Energy Comm. Tech. Report, GAEC-NNRI*, vol. RT-90, 2003.

APPENDIX

SAMPLE INPUT DECK FOR CODES USED

a) Sample MCNP 5 Input deck for GHARR-1 with LEU core.

```
c LEU 335-Pin GHARR1 UO2 Core Based on Generic Materials Compositions
and Impurities for MNSR 2015 Conversion Analyses 7/16/15
c                FIRST RING OF 6 FUEL ELEMENTS
c
6  6  -10.6   -11 -3 4          imp:n=1 tmp=2.5262e-08 $ meat 1  first density =
3.47617
7  12 -6.5000  11 -111 -3 4      imp:n=1 tmp=2.5262e-08 $ clad
8  6  -10.6   -12 -3 4          imp:n=1 tmp=2.5262e-08 $ meat 2
9  12 -6.5000  12 -121 -3 4      imp:n=1 tmp=2.5262e-08 $ clad
10 6  -10.6   -13 -3 4          imp:n=1 tmp=2.5262e-08 $ meat 3
11 12 -6.5000  13 -131 -3 4      imp:n=1 tmp=2.5262e-08 $ clad
12 6  -10.6   -14 -3 4          imp:n=1 tmp=2.5262e-08 $ meat 4
13 12 -6.5000  14 -141 -3 4      imp:n=1 tmp=2.5262e-08 $ clad
14 6  -10.6   -15 -3 4          imp:n=1 tmp=2.5262e-08 $ meat 5
15 12 -6.5000  15 -151 -3 4      imp:n=1 tmp=2.5262e-08 $ clad
16 6  -10.6   -16 -3 4          imp:n=1 tmp=2.5262e-08 $ meat 6
17 12 -6.5000  16 -161 -3 4      imp:n=1 tmp=2.5262e-08 $ clad…
 c MATERIAL 12: Zr-Alloy 4 - adding Equivalent B to Zirc-4 w/o
renormalization
c m12   40000.66c -0.9793 $ Zirconium
c       26000.55c -0.0024 $ Iron
c       24000.50c -0.0013 $ Chromium
c       50000.42c -0.017 $ Tin
c       5010.66c -6.713E-07 $ Equivalent Boron Impurity
c       5011.66c -2.971E-06 $ Equivalent Boron Impurity
c
c    MATERIAL 12: Zr-Alloy 4 - renomalized JRL -8/12/09
m12   40000.66c -0.9792964 $ Zirconium
      26000.55c -0.0024000 $ Iron
      24000.50c -0.0013000 $ Chromium
      50000.42c -0.0169999 $ Tin
       5010.66c -6.713E-07 $ Equivalent Boron Impurity
       5011.66c -2.971E-06 $ Equivalent Boron Impurity
c
c    MATERIAL 13: Zr-Alloy 4 Smeared with Helium Gap
c m13   40000.66c     -0.979298051
c       26000.55c     -0.002399995
c       24000.50c     -0.001299997
```

```
c       50000.42c     -0.016999966
c        5010.66c     -6.71299E-07 $ Equivalent Boron Impurity
c        5011.66c     -2.97099E-06 $ Equivalent Boron Impurity
c        2004.66c     -0.000001652
c
c    MATERIAL 13: Zr-Alloy 4 Smeared with Helium Gap - renomalized JRL -
8/12/09
m13   40000.66c     -0.9792948
      26000.55c     -0.0024000
      24000.50c     -0.0013000
      50000.42c     -0.0169999
       5010.66c     -6.713E-07   $ Equivalent Boron Impurity
       5011.66c     -2.971E-06   $ Equivalent Boron Impurity
       2004.66c     -1.652E-06
c
m25   2004.66c     -1.0000
c
kcode  500000   1.00400  30 330 $ 300M histories for tally files
prdmp  2j 1 1  $ from Benoit to improve efficiency
sdef   erg=d1 rad=d2 ext=d3 pos 0 0 0.0 axs 0 0 1
sp1    -2
si2    0.0  11.50
si3    0.0  23.00
```

b) Sample Input deck for Transient studies using PARET/ANL code.

```
  0 30000                              50
 1.47       10.        10.        20.        30.0       30.0
 0.0001     100.          350.00   1.72370+5    0.006
* PARET:  MNSR   LEU 2 CHANNELS, 2.1 mk transient
!      NCHN    NZ   NR IGEOM IPROP IRXSWT
1001,    -2    21    7     1     1     1
1002,     0     0    6    -1     0    20
```

```
! Assuming 4.3 mm meat od, 0.6mm clad thickness, 335 rods
! Active length 0.23 m
!xxxxx1111111111112222222222223333333333334444444444455555555555566666666666
!      POWER, MW                    ENTHIN       RS
1003,     2.00-6 0.001118921   1.72370+5 -30.00     2.7502002-3
!      RF         RC                        AL       ALDDIN
1004,   2.15000-3   2.15020-3   0.0        0.0        0.2300     0.000
!      ALDDEX      beta
1005,   0.016      8.57000-3   1.41000-4   9.80664     0.002994
!      TRANST                    rho (20C)    GAMMA0
1006,     3000.     0.80       1.0      996.88      0.0
!      GAMMA1     GAMMA2     GAMMA3     GAMMA4     DOPPN      EPS3
1007,   3.00000-7   0.0        0.00       0.00       1.00       0.001
!      DNBQDP     TAUUNB     TAUUTB     ALAMNB     ALAMTB     ALAMFB
1008,   0.00       0.001      0.001      0.05       0.05       0.05
!      HTTCON     HTTEXP
!1009,   1.4        0.33
! try using 0.92 to reduce h
1009,   0.923        0.33
!      PSUBC
1111,   0.033370    1.00        1.00
!             IMODE       IHT
! use CIAE option
1112,     3    1    0    1    0    0
!      RDRATE      TDLAY     POWTP       FLOTP      OPT        POW0
1113,   1.016       0.015     10000.0       0.0       0.        0.0
!      HNCTOP      HNCBOT  FOR NATURAL CONVECTION:HEIGHT ABOVE AND BELOW CORE
!xxxxx1111111111112222222222223333333333334444444444455555555555566666666666
1114,  0.0160      0.0150     2300.     6000.0      1.        1.6
```

```
! fuel k; then fuel rho*cp
! per Floyd July 31/07
2001,   0.0       0.0       167.6       0.00       0.00
2002,   0.0       0.0000+0    2.2400+6    0.00       0.00
! air gap per Floyd July 31/07
2003,   0.0       0.000000    0.0282      0.00       0.00
2004,   0.0       0.0000      1.02000+4   0.00       0.00
! Aluminum clad;
! per Floyd July 31/07
2005,   0.0       0.0       199.7       0.00       0.00
2006,   0.0       0.0000      2.420+6     0.00       0.00
! radial data: 4.3 mm od meat; 0.6 mm clad;
3001,  0.537500-3     5     1   1.000
! minute gap per Floyd 8/1/07
3002,  0.000200-3     6     2   0.00
3003,  0.600000-3     7     3   0.000
4001,   10.9524E-3    21
!xxxxx11111111111122222222222233333333333344444444444455555555555566666666666
!                     RN        BM        ALOSCN      ALOSCX
5100,     4         1.      0.006206    0.008772     80.         80.
!       SIGIN      SIGEX      DVOID      DTMP
5100,   7.66       6.57       1.000      1.000
5101,   0.0000     0.0000      4.505-1     2.400-2
5102,   1.2909      1.00       1.00       1.00
5103,   1.1359      1.00       1.00       1.00
5104,   1.1448      1.00       1.00       1.00
5105,   1.1869      1.00       1.00       1.00
5106,   1.2106      1.00       1.00       1.00
5107,   1.2523      1.00       1.00       1.00
```

5108, 1.2913 1.00 1.00 1.00

5109, 1.3086 1.00 1.00 1.00

5110, 1.3320 1.00 1.00 1.00

5111, 1.3323 1.00 1.00 1.00

5112, 1.3320 1.00 1.00 1.00

5113, 1.3132 1.00 1.00 1.00

5114, 1.2849 1.00 1.00 1.00

5115, 1.2433 1.00 1.00 1.00

5116, 1.1910 1.00 1.00 1.00

5117, 1.1216 1.00 1.00 1.00

5118, 1.0560 1.00 1.00 1.00

5119, 0.9764 1.00 1.00 1.00

5120, 0.9124 1.00 1.00 1.00

5121, 0.8916 1.00 1.00 1.00

5122, 1.0615 1.00 1.00 1.00

!xxxxx1111111111112222222222223333333333334444444444455555555555566666666666

5200, 4 1. 0.006206 0.991228 80. 80.

5200, 7.660 6.570 1.000 1.000

5201, 0.0000 0.0000 4.505-1 2.400-2

5202, 1.0776 1.00 1.00 1.00

5203, 0.9495 1.00 1.00 1.00

5204, 0.9498 1.00 1.00 1.00

5205, 0.9811 1.00 1.00 1.00

5206, 1.0186 1.00 1.00 1.00

5207, 1.0549 1.00 1.00 1.00

5208, 1.0840 1.00 1.00 1.00

5209, 1.1062 1.00 1.00 1.00

5210, 1.1201 1.00 1.00 1.00

5211, 1.1229 1.00 1.00 1.00

```
5212,   1.1185     1.00      1.00      1.00
5213,   1.1030     1.00      1.00      1.00
5214,   1.0778     1.00      1.00      1.00
5215,   1.0441     1.00      1.00      1.00
5216,   1.0022     1.00      1.00      1.00
5217,   0.9518     1.00      1.00      1.00
5218,   0.8945     1.00      1.00      1.00
5219,   0.8359     1.00      1.00      1.00
5220,   0.7868     1.00      1.00      1.00
5221,   0.7800     1.00      1.00      1.00
5222,   0.9291     1.00      1.00      1.00
6001,    3.8546-2  0.12720-1    0.21320  0.31740-1    0.18718    0.11601
6002,     0.40702    0.31101    0.12804     1.4000   2.6014-2     3.8701
!xxxxx1111111111112222222222223333333333334444444444455555555555566666666666
9000,     4   ! 50 second ramp starting at 70.0 sec
9001,      0.0         0.0
9002,      0.0         70.0
9003,      .2450       120.0
9004,      .2450     10000.0
10000,    2
! upflow
! assume some initial flow
!xxxxx1111111111112222222222223333333333334444444444455555555555566666666666
10001,   1.000     0.0         1.000    10000.
11000,    2
11001,  0.0       98.0       0.0        2000.0
12000,    2
12001,  0.0       0.0        0.0        0.0
14000,    6
```

```
14001,  0.010     0.0
14002,  0.0010    60.0
14003,  0.00010   70.0
14004,  0.0010   400.0
14005,  0.0100   600.0
14006,  0.0200  1200.0
16000,    5
!xxxxx1111111111112222222222223333333333334444444444445555555555556666666666666
16001,   0.1      1000      0.0        5.0        1000       20.0
16002,   1.0      1000       70.0       10.0        500       800.0
16003,   50.      1000      600.0
17000,   11
17001,   1.00      0.0       0.75      2.50      0.50        5.00
17002,  0.25       7.50       0.10      9.00      0.05        9.50
17003,  0.01       9.90       0.005     9.95      0.001       9.99
17004,  0.00      10.00       0.00      30000.
18000,    2
18001,   0.0      0.0        -13.0     0.5080
! coolant feedback with temperature
19000,    6
19001,   5.1733-3 293.00
19002,   8.7515-3 303.15
19003,   7.8180-3 323.15
19004,   8.1972-3 333.15
19005,   8.1972-3 373.15
19006,   8.1972-3 473.15
!xxxxx1111111111112222222222223333333333334444444444445555555555556666666666666
! coolant feedback with void
20000,    6
```

20001, 0.45888 0.

20002, 0.39202 0.267

20003, 0.39538 1.029

20004, 0.40250 1.513

20005, 0.40250 3.983

20006, 0.0 100.

c) Sample Input deck for Steady State studies using PLTEMP/ANL code.

GHARR-1, 12 Fuel Type, 335 Fuel Rods Model, Radial Geom, Natural Circulation Card 100
!2345678901234567890123456789012345678901234567890123456789012345678901234567890
! MODELING ASSUMPTIONS:
! Each fuel rod is modeled as a FUEL TUBE having a hole of radius 0.0001 mm
! in the center.
! CHECK THE INLET & EXIT LOSS COEFFICIENTS. They are currently calibrated
! to give the measured coolant temp rise of 13 C during natural circulation
! at a power of 15 kW.
! YOU MUST INPUT AXIAL POWER SHAPE LATER. Uniform assumed now.
! Fuel Tube radii: Ra=0 mm, Rb=0.6 mm, Rc=2.15 mm, Rd=2.75 mm, Rwater=6.216743 mm
! Power per fuel rod=34/335=0.10149 kW, Fueled Length=0.230 m, Inlet Temp=30 C
! Hyd Dia = 4*33594.2284/(Pi*5.5*350 + Pi*231) = 19.83929 mm
! Channel Width = Pi*(Rd + Rwater) = Pi*(2.75 + 6.216743) = 28.16985 mm
! Channel Thickness = Rwater - Rd = 6.216743 - 2.75 = 3.466743 mm
! Chimney Height = Dist from fuel rod upper end to bottom of Aluminum Shim=16 mm
! Fuel Plate Width = Pi*(Rb + Rc) = Pi*(0.6 + 2.15) = 8.63938 mm
! 1 2 3 4 5 6 7 8 9 10 11 12 13 14 15 16 17 18 19 20
51 0 6 12 0 0 1 1 1 0 0 0 0 0 0 1 0 0 0 1 Card 200
1 Card 200A
! 1.0 1.0 1.0 Card 201
30 3 0.005 1.0 1.0 1.0 0 0 Card 300

```
!      1.0       1.0       1.0                                    Card 300A
  1   2       1.0                                                 Card 301
  1   1   1                                                       Card 302
        1.30      1.30      1.31      1.30      1.29      1.29     Card 303
        1.30      1.30      1.30      1.27      1.30      1.27     Card 303
        1.27      1.26      1.26      1.24      1.27      1.28     Card 303
        1.27      1.28      1.28      1.26      1.27      1.27     Card 303
        1.25      1.25      1.24      1.19      1.19      1.17     Card 303
 9.765764E-5 1.983929E-2      0.009      64.0 28.16985E-3 3.466743E-3
Card 304
 9.765764E-5 1.983929E-2      0.230       0.0 28.16985E-3 3.466743E-3
Card 304
 9.765764E-5 1.983929E-2      0.009      64.0 28.16985E-3 3.466743E-3
Card 304
        0.0       0.0       0.0       0.016                      Card 305
  2   0       0.0       0.230   0.5999E-3     180.0      1.55E-3     160.0   Card 306
 9.765764E-7 1.983929E-2 17.27876E-3 17.27876E-3 28.16985E-3 3.466743E-3
Card 307
 9.765764E-5 1.983929E-2 17.27876E-3 17.27876E-3 28.16985E-3 3.466743E-3
Card 307
  8.63938E-3                                                     Card 308
    1.375E-3                                                     Card 308A
      1.175                                                      Card 309
      1.164                                                      Card 309
      1.175                                                      Card 309
      1.162                                                      Card 309
      1.169                                                      Card 309
      1.158                                                      Card 309
      1.159                                                      Card 309
      1.156                                                      Card 309
      1.166                                                      Card 309
      1.160                                                      Card 309
      1.162                                                      Card 309
      1.134                                                      Card 309
      1.128                                                      Card 309
      1.116                                                      Card 309
      1.122                                                      Card 309
      1.114                                                      Card 309
      1.130                                                      Card 309
      1.139                                                      Card 309
      1.130                                                      Card 309
      1.141                                                      Card 309
      1.133                                                      Card 309
```

```
      1.140                                                    Card 309
      1.142                                                    Card 309
      1.139                                                    Card 309
      1.139                                                    Card 309
      1.132                                                    Card 309
      1.095                                                    Card 309
      1.065                                                    Card 309
      1.055                                                    Card 309
      1.052                                                    Card 309
  30   3      0.005       1.0       1.0       1.0   0   0          Card 300
!       1.0       1.0       1.0                                  Card 300A
   1   2       1.0                                               Card 301
   1   1   1                                                     Card 302
       1.17      1.18      1.19      1.18      1.19      1.21     Card 303
       1.22      1.21      1.23      1.23      1.23      1.21     Card 303
       1.22      1.22      1.21      1.22      1.23      1.21     Card 303
       1.18      1.15      1.16      1.13      1.14      1.12     Card 303
       1.12      1.13      1.13      1.14      1.13      1.13     Card 303
 9.765764E-5 1.983929E-2      0.009       64.0 28.16985E-3 3.466743E-3
Card 304
 9.765764E-5 1.983929E-2      0.230        0.0 28.16985E-3 3.466743E-3
Card 304
 9.765764E-5 1.983929E-2      0.009       64.0 28.16985E-3 3.466743E-3
Card 304
        0.0       0.0       0.0      0.016                      Card 305
   2   0        0.0       0.230   0.5999E-3     180.0      1.55E-3     160.0   Card 306
 9.765764E-7 1.983929E-2 17.27876E-3 17.27876E-3 28.16985E-3 3.466743E-3
Card 307
 9.765764E-5 1.983929E-2 17.27876E-3 17.27876E-3 28.16985E-3 3.466743E-3
Card 307
8.63938E-3                                                     Card 308
   1.375E-3                                                    Card 308A
      1.025                                                    Card 309
      0.974                                                    Card 309
      0.972                                                    Card 309
      0.991                                                    Card 309
      1.056                                                    Card 309
!                              POWER     TIN        PRESS
! Power in 6 fuel rods =30/344*344 = 30.00000kW at a reactor power of 34 kW.
     8.0E-6       0.040       0.000 3.400000E-2 30.0       0.12370          Card 500
        0.0         0.0        0.60        0.02                      Card 500
  50      1.0E-4        32.5        0.00        0.00                    Card 600
  21                                                          Card 700
```

```
0.0       1.291                                    Card 701
0.050      1.136                                   Card 701
0.100      1.145                                   Card 701
0.150      1.187                                   Card 701
0.200      1.211                                   Card 701
0.250      1.252                                   Card 701
0.300      1.291                                   Card 701
0.350      1.309                                   Card 701
0.400      1.332                                   Card 701
0.450      1.332                                   Card 701
0.500      1.332                                   Card 701
0.550      1.313                                   Card 701
0.600      1.285                                   Card 701
0.650      1.243                                   Card 701
0.700      1.191                                   Card 701
0.750      1.122                                   Card 701
0.800      1.056                                   Card 701
0.850      0.976                                   Card 701
0.900      0.912                                   Card 701
0.950      0.892                                   Card 701
1.000      1.062                                   Card 701
  0                                              Card 702
```

d) Sample Input deck for Steady State studies using PARET/ANL code.

```
0 30000                                  50
  1.47       10.        10.        20.        30.0       30.0
  0.0001     100.          350.00   1.72370+5    0.006
*  PARET:  MNSR   HEU  2 CHAN  4 mk transient
! inlet and exit K-factors of 80.
!  react.aug02.ciae.k80.inp
!       NCHN    NZ   NR IGEOM IPROP IRXSWT
1001,     -2    21    7     1     1     1
1002,      0     0    6    -1     0    20
! assuming 4.3 mm meat od, 0.6mm clad thickness, 344 rods
! active length 0.23 m
!xxxxx11111111111222222222222333333333333444444444444555555555555
666666666666
```

```
!       POWER, MW                       ENTHIN       RS
1003,     2.00-6 0.001159002   1.72370+5 -30.00     2.7502002-3
!       RF         RC                          AL        ALDDIN
1004,    2.15000-3   2.15020-3   0.0        0.0        0.2300     0.000
!       ALDDEX       beta
1005,    0.016      8.57000-3   5.79000-5   9.80664     0.002994
!       TRANST                        rho (20C)    GAMMA0
1006,     3000.      0.80        1.0       996.88       0.0
!       GAMMA1     GAMMA2     GAMMA3     GAMMA4     DOPPN      EPS3
1007,    2.90000-4   0.0         0.00        0.00        1.00        0.001
!     DNBQDP     TAUUNB     TAUUTB     ALAMNB     ALAMTB     ALAMFB
1008,    0.00        0.001       0.001       0.05        0.05        0.05
!       HTTCON      HTTEXP
!1009,    1.4         0.33
! try using 0.92 to reduce h
1009,    0.923         0.33
!       PSUBC
1111,    0.033370    1.00         1.00
!               IMODE        IHT
! use CIAE option
1112,     3     1     0     1     0     0
!       RDRATE      TDLAY     POWTP        FLOTP      OPT        POW0
1113,    1.016       0.015     10000.0        0.0        0.         0.0
!     HNCTOP      HNCBOT  FOR NATURAL CONVECTION:HEIGHT ABOVE
AND BELOW CORE
!xxxxx11111111111222222222222333333333333444444444444555555555555
666666666666
1114,   0.0160       0.0150      2300.      6000.0       1.         1.6
! fuel k; then fuel rho*cp
! per Floyd July 31/07
2001,    0.0         0.         167.6        0.00        0.00
2002,    0.0         0.0000+0    2.2400+6    0.00        0.00
! air gap per Floyd July 31/07
2003,    0.0         0.000000    0.0282      0.00        0.00
2004,    0.0         0.0000      1.02000+4   0.00        0.00
! Aluminum clad;
! per Floyd July 31/07
2005,    0.0         0.0         199.7        0.00        0.00
2006,    0.0         0.0000      2.420+6      0.00        0.00
! radial data: 4.3 mm od meat; 0.6 mm clad;
3001,  0.537500-3      5     1   1.000
! minute gap per Floyd 8/1/07
3002,  0.000200-3      6     2   0.00
```

```
3003,  0.600000-3     7     3   0.000
4001,   10.9524E-3    21
!xxxxx1111111111112222222222223333333333334444444444445555555555556
666666666666
!                      RN         BM         ALOSCN       ALOSCX
5100,     4          1.      0.006206    0.008772     80.          80.
!       SIGIN       SIGEX       DVOID      DTMP
5100,    7.66        6.57        1.000       1.000
5101,    0.0000      0.0000       1.2412-2   1.2412-2
5102,    1.9417      1.00         1.00        1.00
5103,    1.6408      1.00         1.00        1.00
5104,    1.5150      1.00         1.00        1.00
5105,    1.5397      1.00         1.00        1.00
5106,    1.6145      1.00         1.00        1.00
5107,    1.6959      1.00         1.00        1.00
5108,    1.7714      1.00         1.00        1.00
5109,    1.8367      1.00         1.00        1.00
5110,    1.8816      1.00         1.00        1.00
5111,    1.9125      1.00         1.00        1.00
5112,    1.9247      1.00         1.00        1.00
5113,    1.9186      1.00         1.00        1.00
5114,    1.8950      1.00         1.00        1.00
5115,    1.8544      1.00         1.00        1.00
5116,    1.7984      1.00         1.00        1.00
5117,    1.7241      1.00         1.00        1.00
5118,    1.6351      1.00         1.00        1.00
5119,    1.5370      1.00         1.00        1.00
5120,    1.4353      1.00         1.00        1.00
5121,    1.3540      1.00         1.00        1.00
5122,    1.2728      1.00         1.00        1.00
!xxxxx1111111111112222222222223333333333334444444444445555555555556
666666666666
5200,     4          1.      0.006206    0.991228     80.          80.
5200,    7.660       6.570       1.000       1.000
5201,    0.0000      0.0000       1.2412-2   1.2412-2
5202,    1.1422      1.00         1.00        1.00
5203,    0.9652      1.00         1.00        1.00
5204,    0.8912      1.00         1.00        1.00
5205,    0.9057      1.00         1.00        1.00
5206,    0.9497      1.00         1.00        1.00
5207,    0.9976      1.00         1.00        1.00
5208,    1.0424      1.00         1.00        1.00
5209,    1.0804      1.00         1.00        1.00
```

```
5210,    1.1068      1.00        1.00        1.00
5211,    1.1250      1.00        1.00        1.00
5212,    1.1322      1.00        1.00        1.00
5213,    1.1286      1.00        1.00        1.00
5214,    1.1147      1.00        1.00        1.00
5215,    1.0908      1.00        1.00        1.00
5216,    1.0579      1.00        1.00        1.00
5217,    1.0142      1.00        1.00        1.00
5218,    0.9618      1.00        1.00        1.00
5219,    0.9041      1.00        1.00        1.00
5220,    0.8443      1.00        1.00        1.00
5221,    0.7965      1.00        1.00        1.00
5222,    0.7487      1.00        1.00        1.00
6001,     3.8546-2   0.12720-1     0.21320   0.31740-1     0.18718     0.11601
6002,      0.40702     0.31101     0.12804      1.4000    2.6014-2      3.8701
!xxxxx1111111111112222222222223333333333333444444444444555555555555
666666666666
9000,      4   ! 50 second ramp starting at 70.0 sec
9001,       0.0          0.0
9002,       0.0         70.0
9003,       .2450       120.0
9004,       .2450     10000.0
10000,     2
! upflow
! assume some initial flow
!xxxxx1111111111112222222222223333333333333444444444444555555555555
666666666666
10001,    1.000      0.0         1.000    10000.
11000,     2
11001,   0.0        98.0        0.0         2000.0
12000,     2
12001,   0.0        0.0         0.0         0.0
14000,     6
14001,   0.010      0.0
14002,   0.0010     60.0
14003,   0.00010    70.0
14004,   0.0010    400.0
14005,   0.0100    600.0
14006,   0.0200   1200.0
16000,     5
!xxxxx1111111111112222222222223333333333333444444444444555555555555
666666666666
16001,    0.1       1000       0.0         5.0         1000        20.0
```

```
16002,   1.0      1000      70.0      10.0       500       800.0
16003,   50.      1000      600.0
17000,   11
17001,   1.00      0.0       0.75      2.50      0.50       5.00
17002,  0.25       7.50      0.10      9.00      0.05       9.50
17003,  0.01       9.90      0.005     9.95      0.001      9.99
17004,  0.00       10.00     0.00      30000.
18000,   2
18001,   0.0      0.0        -13.0     0.5080
! coolant feedback with temperature
19000,   6
19001,   5.1733-3 293.00
19002,   8.7515-3 303.15
19003,   7.8180-3 323.15
19004,   8.1972-3 333.15
19005,   8.1972-3 373.15
19006,   8.1972-3 473.15
!xxxxx1111111111112222222222233333333333344444444444555555555555
666666666666
! coolant feedback with void
20000,   6
20001,   0.45888   0.
20002,   0.39202   0.267
20003,   0.39538   1.029
20004,   0.40250   1.513
20005,   0.40250   3.983
20006,   0.0      100.
```